This Page Is Inserted by IFW Operations
and is not a part of the Official Record

BEST AVAILABLE IMAGES

Defective images within this document are accurate representations of the original documents submitted by the applicant.

Defects in the images may include (but are not limited to):

- BLACK BORDERS

- TEXT CUT OFF AT TOP, BOTTOM OR SIDES

- FADED TEXT

- ILLEGIBLE TEXT

- SKEWED/SLANTED IMAGES

- COLORED PHOTOS

- BLACK OR VERY BLACK AND WHITE DARK PHOTOS

- GRAY SCALE DOCUMENTS

IMAGES ARE BEST AVAILABLE COPY.

As rescanning documents *will not* correct images, please do not report the images to the Image Problem Mailbox.

The antihypertensive efficacy of the novel calcium antagonist mibefradil in comparison with nifedipine GITS in moderate to severe hypertensives with ambulatory hypertension.

Lacourciere Y, Poirier L, Lefebvre J, Archambault F, Dalle Ave S, Ward C, Lindberg E.

Hypertension Unit, le Centre Hospitalier de l'Universite Laval, Saint-Foy, Quebec, Canada.

Mibefradil is a novel calcium antagonist that blocks selectively the T-type calcium channels. In this double-blind forced titration study design we compared the effects of mibefradil 50, 100, and 150 mg and nifedipine GITS 30, 60, and 90 mg monotherapies or combined with lisinopril 20 mg in 71 moderate to severe hypertensives (59 men and 12 women) with confirmed ambulatory hypertension. An incremental dose-response effect was observed both in clinic and ambulatory blood pressure parameters during treatment with mibefradil and nifedipine GITS alone and combined with lisinopril. At maximal dosage, patients treated with mibefradil experienced a greater ($P < .05$) reduction in clinic and ambulatory diastolic blood pressures as well as a greater response rate (86% v 69%). Trough:peak ratios for systolic and diastolic blood pressures were > 90% at each dose level. Significant decrease in baseline heart rate was observed with mibefradil 150 mg alone or combined with lisinopril, but no patients experienced clinically significant atrioventricular conduction abnormalities. Adverse events related to vasodilation were more prevalent in the nifedipine GITS group. Consequently, the results of the present study demonstrate that the novel calcium channel blocker mibefradil, either alone or in combination with lisinopril, is effective in reducing clinic and 24-h blood pressures while decreasing heart rate and is well tolerated in patients with moderate to severe hypertension.

Publication Types:

- Clinical Trial
- Randomized Controlled Trial

Evaluating the safety of mibefradil, a selective T-type calcium antagonist, in patients with chronic congestive heart failure.

van der Vring JA, Bernink PJ, van der Wall EE, van Velhuisen DJ, Braun S, Kobrin I.

Martini Ziekenhuis, Groningen, The Netherlands.

Mibefradil is a novel calcium antagonist belonging to a new chemical class of benzimidazolyl-substituted tetraline derivatives. The safety of mibefradil in patients with mild-to-moderate chronic congestive heart failure (CHF) due to coronary heart disease was assessed in a randomized, double-masked, placebo-controlled, multiple-ascending-dose trial in 45 patients. Patients were assigned to receive one of five dose levels (6.25, 12.5, 25, 50, or 100 mg/d) of mibefradil or placebo according to a randomization list. If safety variables remained stable, the subsequent group of patients was randomized to the next higher dose. The safety variables assessed included New York Heart Association class, vital signs, and ejection fraction. Patients were evaluated at baseline and day 8 of the dosing period. Mibefradil did not worsen clinical or cardiac variables. Approximately 23.3% (7 of 30) of the mibefradil-treated patients reported one or more adverse events compared with 13.3% (2 of 15) of the placebo group. The incidence of adverse events was not dose dependent. In summary, short-term oral dosing of mibefradil did not worsen measures of cardiac function in 30 patients with mild-to-moderate CHF.

Publication Types:

- Clinical Trial
- Multicenter Study
- Randomized Controlled Trial

Hemodynamic and cardiac effects of the selective T-type and L-type calcium channel blocking agent mibefradil in patients with varying degrees of left ventricular systolic dysfunction.

Rousseau MF, Hayashida W, van Eyll C, Hess OM, Benedict CR, Ahn S, Chapelle F, Kobrin I, Pouleur H.

Division of Cardiology, University of Louvain, Brussels, Belgium.

OBJECTIVES: This study sought to assess the hemodynamic and cardiac effects of two dose levels of mibefradil in patients with varying degrees of ischemic left ventricular dysfunction. BACKGROUND: Mibefradil is a new, selective T-type and L-type calcium channel blocking agent. Because L-type channel blockade may depress myocardial performance, an invasive hemodynamic study was performed to assess the safety of this agent. METHODS: We performed an open label study, examining the effects of two intravenous doses of mibefradil, selected to produce plasma levels comparable to those measured after oral administration of 50 mg (dose 1: 400 ng/ml) or 100 mg (dose 2: 800 ng/ml) of the drug. Variables studied included the indexes of left ventricular function and neurohormone levels. Patients were stratified according to ejection fraction (EF) (> or = 40%, n = 26; < 40%, n = 24) and the presence (n = 15) or absence (n = 35) of heart failure. RESULTS: In patients with preserved systolic function, dose 1 had no clinically significant hemodynamic effects, but dose 2 decreased mean aortic pressure and systemic vascular resistance (-8.5 mm Hg, -12%, both p < 0.01) and also reduced end-systolic stress and volume, thus improving EF (52% to 58%, p < 0.01). Heart rate tended to decrease. In patients with depressed EF, heart rate decreased significantly with both doses. The effects of dose 1 mimicked those observed after dose 2 in patients with preserved EF. Dose 2 (plasma levels 1,052 +/- 284 ng/ml) still decreased left ventricular systolic wall stress and improved EF (24.0% to 28.5%, p < 0.05) but also significantly depressed the maximal first derivative of left ventricular pressure. Examination of individual pressure-volume loops in two patients with heart failure showed a clear rightward shift of the loop despite a decrease in systolic pressure, suggesting negative inotropy. Neurohormone levels were unchanged at both dose levels and in all subgroups. CONCLUSIONS: Intravenous mibefradil was well tolerated and produced an overall favorable cardiovascular response. However, high plasma concentrations might produce myocardial depression in patients with heart failure, and caution should be exerted in this setting.

Publication Types:

- Clinical Trial
- Multicenter Study

Effects of mibefradil on large and small coronary arteries in conscious dogs: role of vascular endothelium.

Karila-Cohen D, Dubois-Rande JL, Giudicelli JF, Berdeaux A.

Department de Pharmacologie, Faculte de Medecine Paris-Sud, France.

The systemic and coronary hemodynamic effects of mibefradil, a "nondihydropyridine" calcium antagonist acting on both L- and T-type calcium channels, were investigated in chronically instrumented conscious dogs before and after local endothelium removal of the circumflex coronary artery by angioplasty. After intravenous infusion, mibefradil (0.2 mg kg-1 min-1) decreased mean arterial blood pressure (MAP; -15 +/- 1%), increased heart rate (HR; 58 +/- 9%), and coronary blood flow (CBF; 103 +/- 14%) (all $p < 0.05$). Before endothelium removal, mibefradil increased the diameter of the left circumflex epicardial coronary artery (LCX) by 7.8 +/- 1.2% from 3,006 +/- 219 microns, but this dilatory effect was significantly reduced by 69% ($p < 0.001$) and 45% ($p < 0.01$), 3 and 21 days after endothelium removal, respectively. Mibefradil also reduced by 46% ($p < 0.01$) the potent coronary constrictor effect of ergonovine (300 micrograms intravenous bolus). These results demonstrate that mibefradil is a potent dilator of large and small coronary arteries in conscious dogs and that approximately 30% of its dilatory effect on large coronary artery is endothelium-independent. In addition, mibefradil prevents ergonovine-induced epicardial coronary constriction.

Mibefradil, a selective calcium T-channel blocker, in stroke-prone spontaneously hypertensive rats.

Vacher E, Richer C, Fornes P, Clozel JP, Giudicelli.

Departement de Pharmacologie, Faculte de Medecine Paris-Sud, Le Kremlin-Bicetre, France.

Several types of antihypertensive agents, including calcium antagonists, have been reported to prevent stroke and prolong survival in stroke-prone spontaneously hypertensive rats (SHR-SP). We investigated whether mibefradil, a new calcium antagonist acting selectively at the level of T-type calcium channels, would be able to (a) limit or prevent the structural and functional alterations that develop in the cerebral arteries of SHR-SP before stroke and (b) suppress stroke and prolong survival. Mibefradil (30 mg/kg/day) was given orally to young salt-loaded SHR-SP from age 5 weeks to age 20 weeks. Blood pressure (BP) (in conscious animals), diuresis, and proteinuria were determined weekly. After 1012 weeks of treatment, middle cerebral arteries and aortas were removed from randomly selected control and treated SHR-SP. Aortic media thickness and collagen density were evaluated by histomorphometry. Middle cerebral arteries were mounted in a myograph for wall thickness determination and isometric tension recordings. Mibefradil completely prevented stroke and mortality, significantly limited the increase in BP, and opposed the increases in diuresis and proteinuria observed in controls. Simultaneously, mibefradil abolished vascular fibrinoid necrosis formation in the brain and reduced arterial thickening in the cerebral artery as well as in the aorta. The maximal contractile responses of the cerebral arteries to potassium chloride and serotonin were greater in mibefradil-treated animals than in controls, as were the endothelium-dependent relaxant responses. Mibefradil, chronically administered to young SHRSP in a dose that limits the development of hypertension not only prevents stroke and mortality but also affords protection against the vascular structural alterations which develop with age in these animals and preserves or improves the cerebral artery's smooth muscle and endothelial cell functions.

Prevention of neointima formation by mibefradil after vascular injury in rats: comparison with ACE inhibition.

Schmitt R, Clozel JP, Iberg N, Buhler FR.

Pharma Division, F. Hoffmann-La Roche Ltd., Basel, Switzerland.

Cilazapril, an angiotensin-converting enzyme inhibitor, and mibefradil, a selective T-type voltage-operated calcium channel blocker, have been shown to prevent neointima formation after vascular injury. The goal of the present study was to evaluate the mechanism of action of both drugs. For this purpose, the influence of the renin angiotensin system on the effects of mibefradil (30 mg/kg po) and cilazapril (10 mg/kg po) on neointima formation after carotid injury were evaluated in normotensive rats (normal renin angiotensin system) and DOCA hypertensive rats (suppressed renin angiotensin system). In addition, in order to differentiate an effect on cell migration or cell proliferation, both drugs were given either before or after the smooth muscle migration phase. Finally, cilazapril and mibefradil were given in combination. In normotensive rats, mibefradil and cilazapril decreased neointima formation, resulting in neointima/media ratios of 38% (p < 0.05) and 53% (p < 0.01), respectively. However, in DOCA hypertensive rats, mibefradil was active, with a reduction of the neointima/media ratio by 63% (p < 0.001), whereas cilazapril reduced it only slightly (19%) and not significantly. In addition, cilazapril was active only when treatment started before the migration phase (63%, reduction in neointima/media ratio, p < 0.001) but not when started thereafter (13% reduction in neointima/media ratio, n.s.). In contrast, treatment with mibefradil was also active when started after the migration phase (51% reduction in neointima/ media ratio, p < 0.001 when treatment started 1 day before balloon injury and 41%, p < 0.01 when treatment started 5 days after balloon injury). The combination of both drugs was additive (67% reduction in neointima/media ratio, p < 0.001 vs. control). These experiments clearly show that mibefradil and cilazapril have a different mechanism of action after vascular injury. Mibefradil most likely prevents the proliferation of smooth muscle cells. In contrast, cilazapril most likely inhibits the migration of smooth muscle cells. These two different mechanisms of action explain why the effects of both drugs are additive.

Abnormally expressed low-voltage-activated calcium channels in beta-cells from NOD mice and a related clonal cell line.

Wang L, Bhattacharjee A, Fu J, Li M.

Department of Pharmacology, University of South Alabama, College of Medicine, Mobile 36688, USA.

A macroscopic low-voltage-activated (LVA) inward current was found in pancreatic beta-cells isolated from NOD mice. However, this current was not present in nondiabetic prone mouse (e.g., Swiss-Webster) pancreatic beta-cells. We performed pharmacological analyses on this current in NOD insulinoma tumor cells (NIT-1). This cell line was developed from pancreatic beta-cells of a transgenic NOD mouse. The sodium-channel blocker, tetrodotoxin (TTX; 2 micromol/l) had no effect on this LVA current. The amplitudes of currents elicited by a -20 mV test pulse retained similarity when the extracellular sodium concentration was increased from 0 to 115 mmol/l; when the extracellular calcium concentration was decreased from 10 to 2 mmol/l, there was an approximate 50% reduction of this current elicited by a -30 mV test pulse. Neither the L-type calcium-channel blocker, nifedipine (3 micromol/l), nor the N-type calcium-channel blocker, omega-CgTx-GVIA (1 micromol/l), at -30 mV produced an appreciable effect. The T-type calcium-channel blockers, nickel (3 micromol/l) and amiloride (250 micromol/l), effectively reduced the peak of this current. In 2 mmol/l calcium external solution, the threshold of voltage-dependent activation of this calcium current was approximately -65 mV, and the peak current occurred at -20 mV. Half-maximum steady-state inactivation was around -43 mV. The mean time constant of slow deactivating tail currents generated by a preceding 20 mV pulse was 2.53 ms. The intracellular free calcium concentration was two- to threefold higher in NOD mouse pancreatic beta-cells compared with Swiss-Webster pancreatic beta-cells. We concluded that there are LVA calcium channels abnormally expressed in NOD mouse beta-cells. This LVA calcium channel may be factorial to the high cytosolic free calcium concentration observed in these cells, and thereby may contribute to the pathogenesis of NOD mouse beta-cells.

Mechanisms of T-type calcium channel blockade by zonisamide.

Kito M, Maehara M, Watanabe K.

Department of Pediatrics, Minami Seikyo Hospital, Nagoya, Japan.

We investigated the effects of zonisamide, a new antiepileptic drug, on voltage-dependent T-type calcium current (ICa) in cultured neuroblastoma cells of human origin (NB-I). Zonisamide reduced T-type ICa in a concentration-dependent manner without evoking any change in its inactivation kinetics or voltage dependence of action. The mean percent reduction was 38.3 +/- 5.8% at 50 microM. Further, zonisamide shifted the inactivation curve approximately 20 mV negative compared to the control. These resting blocking actions suggest that zonisamide shifts the channel population toward the inactivation state, allowing fewer channels to open during membrane depolarization. The blockade of T-type calcium channels by zonisamide could suppress an important component of inward current that underlies epileptiform cellular bursting, thereby inhibiting the spread of seizure activity.

IN THE UNITED STATES PATENT AND TRADEMARK OFFICE

In the application of:	Examiner: Nirmal S. Basi
Terrance P. SNUTCH, *et al.*	Group Art Unit: 1646
Serial No.: 09/346,794	
Filing Date: 02 July 1999	
For: NOVEL HUMAN CALCIUM CHANNELS AND RELATED PROBES, CELL LINES AND METHODS	

DECLARATION OF DR. TERRANCE SNUTCH

Assistant Commissioner for Patents
Washington, D.C. 20231

Dear Sir:

I, Terrance Snutch, declare as follows:

1.   I am a co-inventor of the subject matter claimed in the above-referenced

application and have been practicing in the field of molecular biology, and specifically in the

field of ion channels, for over 15 years. A copy of my *curriculum vitae* is attached hereto as

Exhibit A. I have published many papers on the structure and function of calcium channels and

am considered one of the leading researchers in this field.

2.   The association of abnormal T-type calcium channel activity with specific

conditions is well known in the art. Enclosed herewith are a number of documents which verify

this. Abnormal T-type activity is associated with a number of cardiac conditions including

pacemaker activity (Hajiwara, *et al., J. Physiol.* (1988) 395:233-253; cardiac hypertrophy (Nuss, *et al., Circ. Res.* (1995) 73:777-782); and hypertension (Self, *et al., J. Vasc. Res.* (1994) 31:359-366). Abnormal T-type calcium function is also associated with neurological diseases wherein neuronal bursts are abnormally fired causing spastic convulsions (Huguenard, *Ann. Rev. Physiol.* (1996) 58:329-348) and thus associated with epilepsy (Tsakiridou, *et al., J. Neuro. Sci.* (1995) 15:3110-3117; Coulter, *et al., Brit. J. Pharmacol.* (1990) 100:800-806). Abnormal function of the T-type calcium ion channel is also associated with impaired fertility because of its effect on hormone secretion (Rossier, *et al., Endocrinology* (1966) 137:4817-4826; Arnoult, *et al., Proc. Natl. Acad. Sci. USA* (1996) 93:13004-13009). Copies of these documents are attached hereto. Thus the conditions associated with abnormal T-calcium channel function are well established and agonists and antagonists of T-type calcium channels are useful in treating these conditions.

3. There are several T-type calcium channels found in a single individual which vary slightly in structure and demonstrably in terms of their distribution among various tissues. This, however, does not affect the usefulness of screening assays for agonists and antagonists. The particular T-type calcium channel involved in a particular condition may depend on its tissue distribution; for instance, T-type channels found in the nervous system are associated with epilepsy and neurological diseases in general where spastic convulsions are involved. However, it is not necessary to understand which particular T-type calcium channel is being used in a screen for compounds that would be useful in treating, for example, these convulsive conditions because of the similarity in the binding specificity of all T-type channels. In very simple terms, compounds which are found to inhibit or stimulate the activity of nervous T-type channels will also inhibit or stimulate the activity of T-type channels found in other tissues. Thus, any arbitrarily chosen T-type channel could be expressed in a cell line for use in screening assays to identify agonists or antagonists and the agonists or antagonists would be useful in treating the conditions associated with any T-type channel. As noted above, abnormal T-type activity is associated with a number of cardiac conditions, with hypertension, with neurological diseases involving spastic convulsions, and with impaired fertility. An agonist or antagonist identified with regard to any T-type channel would be useful in any and all of these conditions.

4. This pattern of similar binding activity among all T-type channels can be analogized to such a pattern among L-type channels. All of the T-type channels have similar

2

behaviors in that they activate at low membrane potential, have small single channel conductance, have negative steady state inactivation properties, and contribute to spike firing patterns and rhythmic bursting processes. Analogous to the T-type channel another type of channel linked by similar behaviors is the L-type. There are several α_1 subunits associated with various L-type channels - *i.e.*, α_{1S}, α_{1C}, and α_{1D} and each is encoded by a distinct gene and exhibits a distinct distribution pattern. For example, α_{1S} is in skeletal muscle; α_{1C} is in neurons and cardiac and smooth muscle; and α_{1D} is found in neurons and endocrine cells. They can be discriminated from all other types of calcium channels by their common sensitivity to 1,4-dihydropyridines. Thus, any one of these genes could be used to generate an L-type calcium channel for use in a cell-based assay to identify interacting compounds. These interacting compounds bind to all L-type channels and thus are useful in treating conditions related to any one of them.

I declare that all statements made herein of my own knowledge are true and that all statements made on information and belief are believed to be true; and further, that these statements are made with the knowledge that willful, false statements and the like so made are punishable by fine or imprisonment or both, under Section 1001 of Title 18 of the United States Code and that such willful false statements may jeopardize the validity of the application or any patent issued thereon.

Executed at _____VANCOUVER, B.C.___ on __10__ July 2001.

_____
Terrance Snutch

sd-42097

concentrations of L-Arg (5 to 100 mM) to muscles treated with L-NMMA and TNF-α resulted in a more pronounced negative inotropic effect than that seen with TNF-α alone [19 ± 4% of baseline tension with TNF-α and L-Arg as compared to 59 ± 7% of baseline tension with TNF-α alone ($P < 0.01$, $n = 6$; Student's two-tailed t test)] (Fig. 4A). This suggests that L-Arg enhanced the negative inotropic effect of TNF-α by providing additional substrate for NO production. This effect was also greater than that seen with L-Arg (100 mM) alone (31 ± 6% of baseline tension; $P < 0.01$, $n = 6$; Student's two-tailed t test). The addition of L-Arg (100 mM) to muscles treated with L-NMMA and IL-6 reduced tension to 35 ± 3% (Fig. 4B). The addition of L-Arg (100 mM) to muscles treated with L-NMMA and IL-2 reduced tension to 11 ± 10% of baseline (Fig. 4C). All of these inotropic effects were completely reversed within 30 min after the cytokines or other agents were washed away (Fig. 4, A through C). Removal of the endothelium did not alter the negative inotropic responses of the papillary muscles to cytokines (Fig. 4, A through C).

Cytokines increase the amount of NO in noncardiac tissues by inducing the transcription of an inducible NO synthase (13–16). The rapid onset and reversibility of the effects seen in this report argue against an effect requiring gene transcription. The negative inotropic effects of these cytokines in the papillary muscle preparation appear to result from enhanced activity of a constitutive NO synthase enzyme in the myocardium.

The observed inotropic effects of pro-inflammatory cytokines raise the possibility that they participate in reversible, postischemic myocardial depression ("stunning"). Myocardial stunning frequently occurs after cardiopulmonary bypass and may complicate successful recovery from cardiac surgery (5–9). We found elevated concentrations of IL-6 (1800 to 4000 U/ml) in bronchoalveolar fluid from patients after cardiopulmonary bypass (18). IL-6 also reversibly decreased tension generated by pectinate muscles removed from patients at the time of surgery (18). These preliminary observations in patients support the clinical relevance of our findings with the Syrian hamster papillary muscle preparation. Thus, the regulation of pro-inflammatory cytokines and myocardial NO synthase may provide new therapeutic strategies for the management of cardiac patients.

REFERENCES AND NOTES

1. J. Van Damme et al., J. Exp. Med. 165, 914 (1987).
2. R. D. Garman, K. A. Jacobs, S. C. Clark, D. H. Raulet, Proc. Natl. Acad. Sci. U.S.A. 84, 7629 (1987).
3. A. Naldini, W. R. Fleischmann, Z. K. Ballas, K. D. Klimpel, G. R. Klimpel, J. Immunol. 139, 1880 (1987).
4. B. Beutler and A. Cerami, Annu. Rev. Immunol. 7, 625 (1989).
5. R. Engler and J. W. Covell, Circ. Res. 61, 20 (1987).
6. B. R. Lucchesi, S. W. Werns, J. C. Fantone, J. Mol. Cell. Cardiol. 21, 1241 (1989).
7. L. O. Go et al., Am. J. Physiol. 255, H1188 (1988).
8. W. Westlin and K. M. Mullane, Circulation 80, 1828 (1989).
9. K. M. Mullane, W. Westlin, R. Kraemer, Ann. N.Y. Acad. Sci. 524, 103 (1988).
10. R. M. J. Palmer, D. S. Ashton, S. Moncada, Nature 333, 664 (1988).
11. L. J. Ignarro, G. M. Buga, K. S. Wood, R. E. Byrns, G. Chaudhuri, Proc. Natl. Acad. Sci. U.S.A. 84, 9265 (1987).
12. S. Moncada et al., J. Cardiovasc. Pharmacol. 17 (suppl. 3), S1 (1991).
13. S. J. Green, C. A. Nacy, M. S. Meltzer, J. Leukocyte Biol. 50, 93 (1991).
14. D. J. Stuehr, H. J. Cho, N. S. Kwon, M. F. Weise, C. F. Nathan, Proc. Natl. Acad. Sci. U.S.A. 88, 7773 (1991).
15. L. Li, R. G. Kilbourn, J. Adams, I. J. Fidler, Cancer Res. 51, 2531 (1991).
16. S. S. Gross, E. A. Jaffe, R. Levi, R. G. Kilbourn, Biochem. Biophys. Res. Commun. 178 (no. 3), 823 (1991).
17. A. M. Shah, J. A. Smith, M. J. Lewis, J. Cardiovasc. Pharmacol. 17 (suppl. 3), S251 (1991).
18. B. G. Hattler and M. S. Finkel, paper presented at the 20th Annual Meeting of the Keystone Symposia on Molecular and Cellular Biology, Steamboat Springs, CO, 1 April 1991.
19. M. S. Finkel, L. Shen, R. C. Romeo, C. V. Oddis, G. Salama, J. Cardiovasc. Pharmacol. 19, 610 (1992).
20. A. I. De'Agostini, S. C. Watkins, H. S. Slayter, H. Youssoufian, R. D. Rosenberg, J. Cell Biol. 111, 1293 (1991).
21. Supported by awards from the American Heart Association, (Western) Pennsylvania Affiliate, the Sarah and David Weis Cardiovascular Research Fellowship, and NIH grant No. GM-37753. We thank B. A. Busch for assistance in the preparation of this manuscript.

Structure and Functional Expression of an ω-Conotoxin–Sensitive Human N-Type Calcium Channel

Mark E. Williams, Paul F. Brust, Daniel H. Feldman, Saraswathi Patthi, Susan Simerson, Azarnoush Maroufi, Ann F. McCue, Gönül Veliçelebi, Steven B. Ellis, Michael M. Harpold*

N-type calcium channels are ω-conotoxin (ω-CgTx)–sensitive, voltage-dependent ion channels involved in the control of neurotransmitter release from neurons. Multiple subtypes of voltage-dependent calcium channel complexes exist, and it is the α_1 subunit of the complex that forms the pore through which calcium enters the cell. The primary structures of human neuronal calcium channel α_{1B} subunits were deduced by the characterization of overlapping complementary DNAs. Two forms (α_{1B-1} and α_{1B-2}) were identified in human neuroblastoma (IMR32) cells and in the central nervous system, but not in skeletal muscle or aorta tissues. The α_{1B-1} subunit directs the recombinant expression of N-type calcium channel activity when it is transiently co-expressed with human neuronal β_2 and α_{2b} subunits in mammalian HEK293 cells. The recombinant channel was irreversibly blocked by ω-CgTx but was insensitive to dihydropyridines. The $\alpha_{1B-1}\alpha_{2b}\beta_2$-transfected cells displayed a single class of saturable, high-affinity (dissociation constant = 55 pM) ω-CgTx binding sites. Co-expression of the β_2 subunit was necessary for N-type channel activity, whereas the α_{2b} subunit appeared to modulate the expression of the channel. The heterogeneity of α_{1B} subunits, along with the heterogeneity of α_2 and β subunits, is consistent with multiple, biophysically distinct N-type calcium channels.

Voltage-dependent Ca²⁺ channels are multisubunit complexes through which extracellular Ca²⁺ enters excitable cells. In rabbit skeletal muscle, four tightly coupled subunits, α_1, α_2, β, and γ, make up the channel complex (1). The primary structure of each subunit has been determined and α_1, α_2, and β cDNAs have been used to characterize transcripts expressed in other tissues (2). The α_1 and β subunits are each encoded by a gene family, including at least five distinct genes for α_1 subunits and three genes for β subunits (3–6). Primary transcripts of each of the α_1 genes, the α_2 gene, and two of the β genes have been shown to yield multiple, structurally distinct, subunits by means of differential processing (6–9). Expression studies have shown that the α_1 subunit forms the pore through which Ca²⁺ enters the cell (10, 11).

On the basis of biophysical and pharmacological characteristics, three subtypes of neuronal, high-voltage–activated Ca²⁺ channels (L-, N-, and P-type) have been proposed (2). These high-voltage–activated

SIBIA, Inc., 505 Coast Boulevard South, La Jolla, CA 92037.

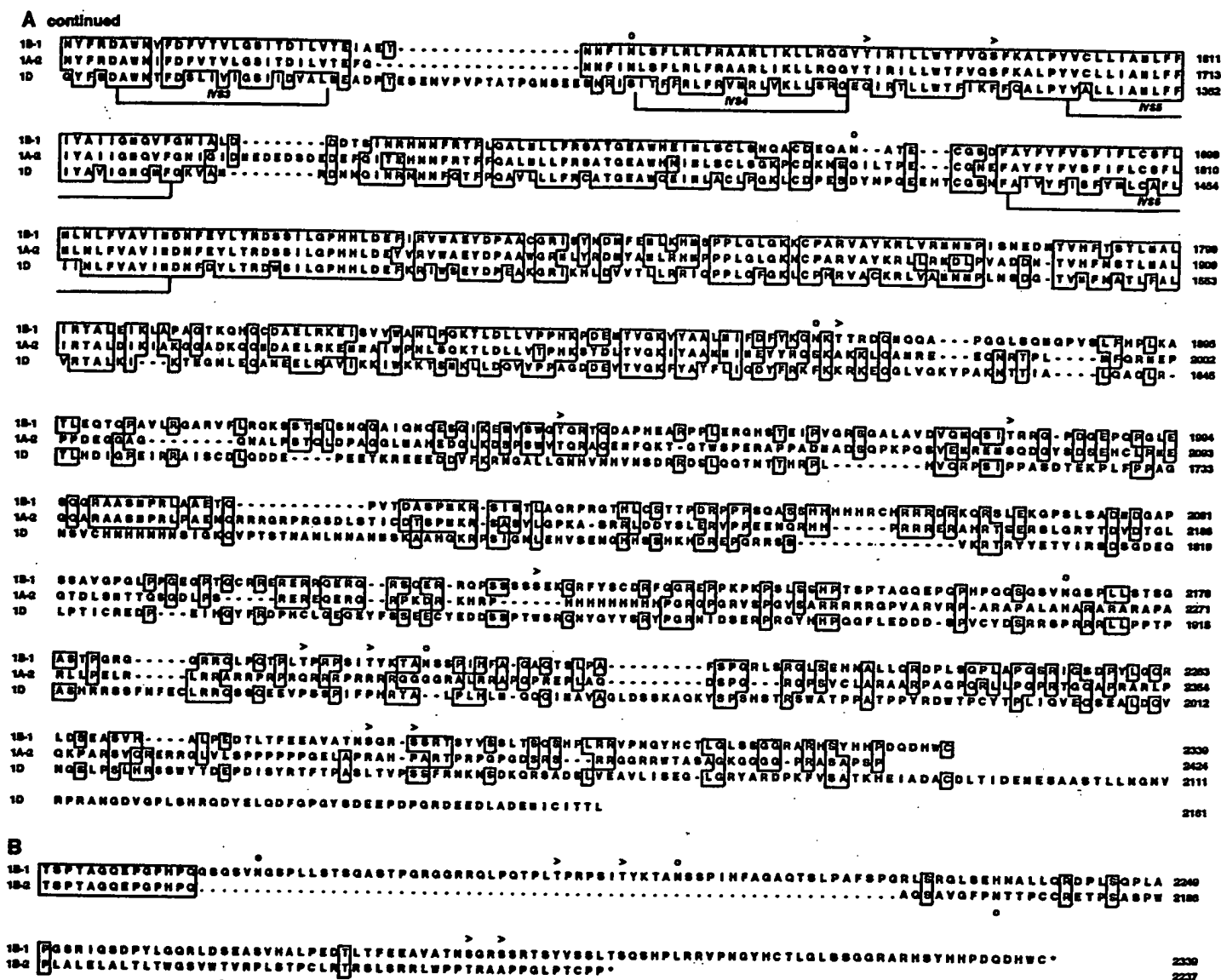*To whom correspondence should be addressed.

A

A continued

[Figure: amino acid sequence alignment panels A and B]

Fig. 1. Alignment of α_1 subunit deduced amino acid sequences. The nucleotide sequences have been deposited in GenBank (accession numbers M94172 and M94173 for α_{1B-1} and α_{1B-2}, respectively). The number of the amino acid residue at the end of each line is given. Abbreviations for the amino acid residues are: A, Ala; C, Cys; D, Asp; E, Glu; F, Phe; G, Gly; H, His; I, Ile; K, Lys; L, Leu; M, Met; N, Asn; P, Pro; Q, Gln; R, Arg; S, Ser; T, Thr; V, Val; W, Trp; and Y, Tyr. Identical residues at one position in at least two of the sequences are enclosed in boxes. Potential N-glycosylation (o), cyclic adenosine monophosphate (AMP)–dependent phosphorylation (<), and protein kinase C phosphorylation (>) sites (36) are shown. (**A**) Alignment of functional, neuronal α_1 subunits; the amino acid sequences of the human neuronal Ca^{2+} channel α_{1B-1} (1B-1), the human neuronal α_{1D} (1D) (8), and the rabbit brain BI-2 (1A-2) (11) are shown. BI-2 is designated 1A-2 because it is a rabbit homolog of the rat brain class A gene (4). The numbering begins with the proposed initiating methionine. The putative transmembrane segments S1 through S6 in each of the repeats I through IV are shown (brackets). (**B**) Alignment of α_{1B-1} and α_{1B-2} sequences through the region of the insertion-deletion (21). The deduced amino acid sequence of the 187-nt insertion (α_{1B-1} nt 6490 to 6676; Gly^{2164} to Gly^{2226}) is shown.

subtypes are most readily distinguished pharmacologically. The neuronal L-type channel is dihydropyridine (DHP)-sensitive and, in some cases, reversibly blocked by ω-conotoxin (ω-CgTx) (12, 13), the N-type channel is DHP-insensitive and irreversibly blocked by ω-CgTx (14), and the P-type channel is both DHP- and ω-CgTx–insensitive but is sensitive to toxins in venom from funnel web spiders (15). Recently, recombinant expression of neuronal Ca^{2+} channels was used to identify a high-voltage–activated, DHP-sensitive Ca^{2+}

channel that was reversibly blocked by ω-CgTx (classified as an L-type channel) (8) and a DHP-, ω-CgTx–insensitive Ca^{2+} channel (possibly a P-type channel) (11). Co-expression of α_1 and β subunits is necessary for substantial functional expression of both Ca^{2+} channel subtypes, whereas addition of an α_2 subunit increases the magnitude of the functional response.

Much evidence indicates that DHP-insensitive N-type Ca^{2+} channels that are irreversibly blocked by ω-CgTx are responsible for the voltage-activated release of

neurotransmitters in many neurons (16). In addition, ω-CgTx binding sites have been localized to the frog neuromuscular presynaptic membrane (17) and to organized, single clusters coincident with synaptic contact sites in hippocampal neurons (18). Furthermore, ω-CgTx binding sites on the presynaptic membrane of the frog neuromuscular terminal align precisely with active zones where vesicular exocytosis of neurotransmitters occurs (16, 17). Finally, ω-CgTx irreversibly blocks Ca^{2+} currents recorded directly from presynaptic termi-

nals (19). We report here the complete amino acid sequence of a human neuronal α_1 subunit (designated α_{1B}) that mediates N-type voltage-dependent Ca^{2+} channel activity, which is irreversibly blocked by ω-CgTx when transiently co-expressed with the human neuronal α_{2b} and β_2 subunits (8) in human embryonic kidney (HEK) 293 cells. The transfected cells bind ω-CgTx with high affinity.

We previously reported the isolation of cDNAs that encode the α_1 subunit of the rabbit skeletal muscle DHP-sensitive, L-type Ca^{2+} channel (3). These cDNAs were used as probes to isolate overlapping cDNAs encoding a complete human neuronal α_{1B} subunit (20). The translation initiation site was assigned to the first in-frame methionine codon, and no upstream in-frame nonsense codon was identified (Fig. 1A). Two isoforms of α_{1B}, α_{1B-1} and α_{1B-2}, that differ at their COOH-termini were identified (Fig. 1B). The α_{1B-1} subunit is comprised of 2339 amino acids and yields a calculated molecular weight of 262,494, whereas the α_{1B-2} subunit is comprised of 2237 amino acids and yields a calculated molecular weight of 251,757. These isoforms were identified by polymerase chain reaction (PCR) analysis (21) and revealed a deletion that produces α_{1B-2}, which likely results from alternative selection of a splice acceptor. This insertion-deletion that produces different COOH-termini is similar to the processing of putative rabbit α_{1A} gene transcripts encoding the rabbit BI-1 and BI-2 isoforms that mediate DHP-, ω-CgTx–insensitive high-voltage–activated Ca^{2+} channel activity (11). The α_{1B} sequence is 94.5% identical to the previously reported 164–amino acid sequence deduced from a rat brain class B partial cDNA (4) and has the same transmembrane topology as described previously for other Ca^{2+} channel α_1 subunits (7).

The deduced amino acid sequences of two different neuronal α_1 subunits, the human α_{1D} (8) and the rabbit BI-2 (11), are shown aligned with the human α_{1B-1} sequence (Fig. 1A). The α_{1B-1} amino acid sequence is 64.1% and 43.0% identical to the BI-2 and α_{1D} sequences, respectively. The sequence identity is relatively well conserved through the four repeating domains, 72.6% and 50.7% for the α_{1B-1}/BI-2 and the α_{1B-1}/α_{1D} pairs, respectively. Both of the DHP-insensitive α_1 subunits, human neuronal α_{1B-1} and rabbit neuronal BI-2, have characteristic large putative cytoplasmic loops between the IIS6 and IIIS1 transmembrane domains. PCR analysis performed on RNAs isolated from IMR32 cells and several human primary tissues with α_{1B-1}- and α_{1B-2}-specific oligonucleotides identified α_{1B-1} and α_{1B-2} transcripts in IMR32 cells and in each of the human

central nervous system (CNS) tissues tested, including hippocampus, habenula, and thalamus but not in human skeletal muscle or aorta tissues (22).

The transient expression of the human neuronal α_{1B-1}, α_{2b}, and β_2 (8) subunits was studied in HEK293 cells (23). Transfected cells were examined for inward Ba^{2+} currents (I_{Ba}) mediated by voltage-dependent Ca^{2+} channels (24). Cells cotransfected with the α_{1B-1}, α_{2b}, and β_2 cDNAs expressed high-voltage–activated Ca^{2+} channels (Fig. 2). I_{Ba} first appeared when the membrane was depolarized from a holding potential of -90 mV to -20 mV and peaked in magnitude at 10 mV. Thirty-nine of 95 cells (12 independent transfections) had I_{Ba} that ranged from 30 to 2700 pA, with a mean of 433 pA. The mean current density was 26 pA/pF, and the highest density was 150 pA/pF (25). The I_{Ba} typically increased by 2- to 20-fold during the first 5 min of recording. Repeated depolar-

Fig. 2. Voltage dependence and kinetics of I_{Ba} expressed in HEK293 cells transfected with α_{1B-1}, α_{2b}, and β_2 cDNAs (23). **(A)** Family of currents evoked at test voltages from -30 to 60 mV, from a holding potential of -90 mV. **(B)** Peak current-voltage relations measured from the currents in (A).

Fig. 3. Holding potential sensitivity of I_{Ba} expressed in HEK293 cells transfected with α_{1B-1}, α_{2b}, and β_2 cDNAs (23). Peak current-voltage (I-V) relations measured from voltage steps delivered from different holding potentials (-90 mV, □; -70 mV, ○; -50 mV, △; return to -90 mV, ▽).

izations during long recordings often revealed rundown of I_{Ba} usually not exceeding 20% within 10 min. I_{Ba} typically activated within 10 ms and inactivated with both a fast time constant ranging from 46 to 105 ms and a slow time constant ranging from 291 to 453 ms ($n = 3$). Inactivation showed a complex voltage dependence, such that I_{Ba} elicited at ≥ 20 mV inactivated more slowly than I_{Ba} elicited at lower test voltages, possibly a result of an increase in the magnitude of slow compared to fast inactivation components at higher test voltages.

Recombinant $\alpha_{1B-1}\alpha_{2b}\beta_2$ channels were sensitive to holding potential (Fig. 3). Steady-state inactivation of I_{Ba}, measured after a 30- to 60-s conditioning at various holding potentials, was approximately 50% at holding potentials between -60 and -70 mV and approximately 90% at -40 mV. Recovery of I_{Ba} from inactivation was usually incomplete, measuring 55 to 75% of the original magnitude within 1 min after the holding potential was returned to more negative potentials, possibly indicating some rundown or a slow recovery rate.

Recombinant $\alpha_{1B-1}\alpha_{2b}\beta_2$ channels were also blocked irreversibly by ω-CgTx concentrations ranging from 0.5 to 10 μM during the time scale of the experiments (Fig. 4). Application of 5 μM toxin ($n = 7$) blocked the activity completely within 2 min, and we observed no recovery of I_{Ba} after washing ω-CgTx from the bath for up to 15 min. Cd^{2+} blockage (50 μM) was rapid, complete, and reversible; the DHPs Bay K 8644 (1 μM; $n = 4$) or nifedipine (5 μM; $n = 3$) had no discernable effect.

Cells cotransfected with cDNAs encoding α_{1B-1}, α_{2b}, and β_2 subunits predominantly displayed a single class of saturable, high-affinity ω-CgTx binding sites (26) (Fig. 5). The determined dissociation constant (K_d) value (Fig. 5) was 54.6 ± 14.5 pM ($n = 4$). Cells transfected with the vector containing only β-galactosidase cDNA or $\alpha_{2b}\beta_2$ cDNA showed no specific binding. The binding capacity (B_{max}) of the $\alpha_{1B-1}\alpha_{2b}\beta_2$-transfected cells was 28,710 ± 11,950 sites per cell ($n = 4$).

These results demonstrate that α_{1B-1}-$\alpha_{2b}\beta_2$-transfected cells express high-voltage–activated, inactivating Ca^{2+} channel activity that is irreversibly blocked by ω-CgTx, insensitive to DHPs, and sensitive to holding potential. The activation and inactivation kinetics and voltage sensitivity of the channel formed in these cells are generally consistent with previous characterizations of neuronal N-type Ca^{2+} channels (27, 28). Furthermore, the K_d value determined for ω-CgTx binding is in agreement with previously reported values (29).

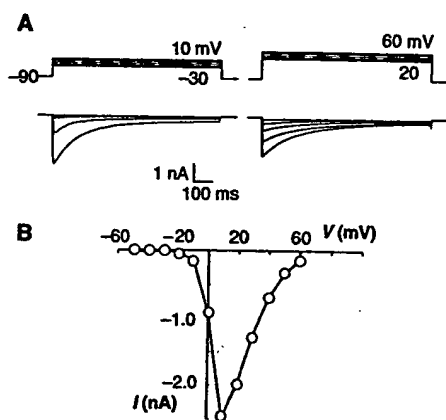The binding characteristics of ω-CgTx to HEK293 cells transiently expressing various subunit combinations were determined
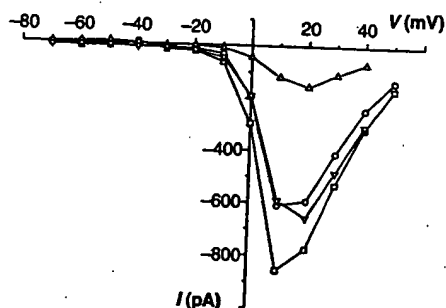
from saturation binding analysis (Table 1). Each recombinant cell type displayed a single class of binding sites similar to the $\alpha_{1B-1}\alpha_{2b}\beta_2$-transfected cells, with K_d values ranging from 38.8 ± 13.1 pM to 76.1 ± 15.5 pM. The binding affinity of the recombinant cell types for ω-CgTx agrees well with that determined for intact IMR32 cells (36.5 ± 6.2 pM) (Table 1) but is different from measurements derived from crude homogenates of IMR32 cells (30).

There were significant differences in the receptor densities of the four recombinant cell types (Table 1). The B_{max} for ω-CgTx binding in $\alpha_{1B-1}\alpha_{2b}\beta_2$-type cells was approximately ten times greater than that in $\alpha_{1B-1}\alpha_{2b}$- and α_{1B-1}-type cells. The estimate for the binding capacity of the IMR32 cells correlates well with a previous report (30). The comparison of the B_{max} values suggests that the ω-CgTx–binding α_{1B-1} subunit is more efficiently expressed on the cell surface when co-expressed with the α_{2b} and β_2 subunits. Similarly, efficient expression of heteromeric protein complexes on the cell surface, such as nicotinic acetylcholine receptors, has been shown to require subunit assembly (31).

We performed whole cell recordings of HEK293 cells transfected with the cDNA encoding α_{1B-1} or with cDNAs encoding α_{1B-1} and α_{2b} or β_2 to assess functional contributions of the various subunits to the N-type channel activity. Currents recorded from $\alpha_{1B-1}\beta_2$-transfected cells were observed at a frequency comparable to that of the $\alpha_{1B-1}\alpha_{2b}\beta_2$-transfected cells (16 of 46 cells; five independent transfections), consistent with a B_{max} of approximately 12,000 receptors per cell (Table 1). These currents resembled those observed in $\alpha_{1B-1}\alpha_{2b}\beta_2$-transfected cells, having similar current-voltage (I-V) curves, inactivation kinetics, and sensitivity to holding potential. Furthermore, $\alpha_{1B-1}\beta_2$-mediated currents were irreversibly blocked by ω-CgTx (5 μM; $n = 3$). However, currents in $\alpha_{1B-1}\beta_2$-transfected cells were generally smaller in magnitude than those observed in $\alpha_{1B-1}\alpha_{2b}\beta_2$ cells and never exceeded 205 pA (15 pA/pF), with a mean of 91 pA (5.6 pA/pF). In contrast, currents in $\alpha_{1B-1}\alpha_{2b}\beta_2$-transfected cells exceeded 200 pA in 57% of the cells tested (25).

Of 23 cells studied that were transfected with only α_{1B-1} (three independent transfections), two had small (20 to 40 pA) rapidly inactivating ($\tau = \sim$20 ms) currents that were reversibly blocked by ω-CgTx. A similar current was detected in 1 of 11 $\alpha_{1B-1}\alpha_{2b}$-transfected cells, whereas none of the untransfected HEK293 cells ($n = 17$) or HEK293 cells transiently expressing the α_{2b} and β_2 subunits ($n = 17$) displayed such currents. These results together with the relatively small B_{max} values observed in

α_{1B-1}-only and $\alpha_{1B-1}\alpha_{2b}$-transfected cells (<2650 receptors per cell) further support the importance of the β subunit in the formation of functional N-type Ca^{2+} channels.

N-type Ca^{2+} channels characterized from different cell preparations have biophysically distinct properties that have made it difficult to distinguish N- and

Fig. 4. Effect of ω-CgTx on I_{Ba} expressed in HEK293 cells transfected with α_{1B-1}, α_{2b}, and β_2 cDNAs (23). (A) Plot of peak current magnitude versus time before, during (hatched bar), and after (open bar) application of 5 μM ω-CgTx. Test pulses (10 mV; holding potential = $-$90 mV) were delivered every 15 s before and during toxin application. Pulses were resumed every 30 s after recording of current-voltage relations from which only the current measured at 10 mV is shown. Similar results were obtained with the three concentrations of ω-CgTx tested: 0.5 μM ($n = 3$), 5 μM ($n = 7$), and 10 μM ($n = 6$). (B) Example recordings made at points 1 to 4 of (A).

Fig. 5. Binding of ^{125}I-ω-CgTx. HEK293 cells were cotransfected with the α_{1B-1}, α_{2b}, and β_2 cDNAs (23) and assayed for specific binding of ^{125}I-ω-CgTx as a function of increasing concentration of ^{125}I-ω-CgTx (26); 2×10^5 cells were used in the assay mixture. (Inset) Scatchard analysis of the data. B, bound; F, free.

L-type currents on the basis of inactivation properties. N-type Ca^{2+} channels were first described in chicken sensory neurons as high-voltage–activated Ca^{2+} channels that could be activated only from strongly negative holding potentials and inactivated within tens of milliseconds (27). Current remaining after decay of the inactivating component or currents activated from holding potentials ≥ -40 mV were believed to represent L-type channel activity. N-type Ca^{2+} channels have since been found to inactivate slowly and incompletely in some neuronal types (32). The range of inactivation rates observed in different tissues may be a result of a combination of factors, including distinct combinations of variant channel subunits and different states of regulation. Recent single channel analysis indicates that individual N-type channels can switch between transient and long-lasting modes of gating (33). Our whole cell data that show biphasic decay of a recombinantly expressed N-type Ca^{2+} channel are consistent with a population of channels that exhibit different gating modes.

Recent biochemical studies on brain ω-CgTx receptors have revealed proteins on SDS–polyacrylamide gel electrophoresis of a relative molecular mass consistent with α_1, α_2, and β subunits (29), although additional uncharacterized bands were also observed. Molecular biological evidence indicates that multiple α_1, α_2, and β transcripts, including α_{1B}, α_{2b}, and β_2 mRNAs, are co-expressed in IMR32 cells and hippocampal tissue (8), both sources of ω-CgTx binding sites (18, 30). The recombinant expression of α_{1B-1}, α_{2b}, and β_2 subunits to produce ω-CgTx–sensitive N-type channel activity confirms that an α_{1B} gene product mediates this activity. The functional necessity of a β subunit and modulation by an
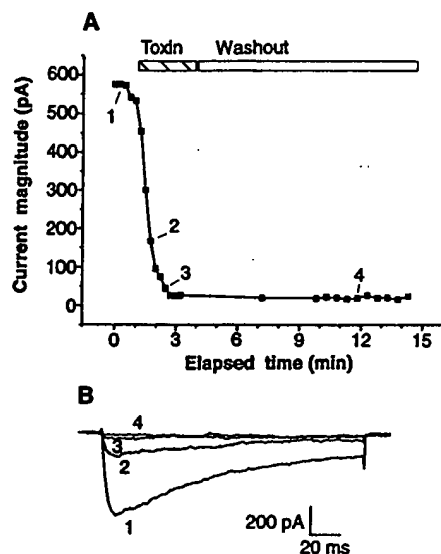
Table 1. Summary of Scatchard analysis of ω-CgTx binding to intact cells. HEK293 cells transfected with the indicated subunit cDNAs and IMR32 cells induced with dibutyryl cyclic AMP and bromodeoxyuridine (28) were assayed for saturation of specific ω-CgTx binding, and the data were analyzed by the Scatchard method (26). The B_{max} values determined from Scatchard analysis were corrected for transfection efficiency.

Cell line	K_d (pM)	B_{max} (sites/cell)
$\alpha_{1B-1}\alpha_{2b}\beta_2$	54.6 ± 14.5	$28,710 \pm 11,950$ ($n = 4$)
$\alpha_{1B-1}\beta_2$	38.8 ± 13.1	$11,860 \pm 5,910$ ($n = 4$)
$\alpha_{1B-1}\alpha_{2b}$	76.1 ± 15.5	$2,650 \pm 620$ ($n = 4$)
α_{1B-1}	59.1 ± 15.5	$2,085 \pm 880$ ($n = 4$)
IMR32	36.5 ± 6.2	$6,770 \pm 615$ ($n = 2$)

α_2 subunit are consistent with the recombinant functional expression of other α_1 subtypes (8, 11), although expression of α_{1B-1} alone appears sufficient for ω-CgTx binding.

Our results suggest that multiple subtypes of the N-type channel might exist as a result of the heterogeneity of the subunits that comprise the channel complex. Co-expression of three different β gene products with the rabbit cardiac (α_{1C}) subunit alters the channel properties and thus indicates that subunit composition can determine distinct, voltage-dependent Ca^{2+} channels (6). At least two forms each of α_{1B}, α_2, and β transcripts expressed in the brain are products of differential processing (6, 8, 34). This heterogeneity of the α_{1B}, α_2, and β subunits is consistent with biophysically distinct N-type channels characterized from different cell preparations. Recombinant expression of each of the α_{1B}, α_2, and β forms might reveal multiple N-type channels and the functional consequence of various subunit combinations (35).

REFERENCES AND NOTES

1. K. P. Campbell, A. T. Leung, A. H. Sharp, *Trends Neurosci.* 11, 425 (1988).
2. R. J. Miller, *J. Biol. Chem.* 267, 1403 (1992).
3. S. B. Ellis *et al.*, *Science* 241, 1661 (1988).
4. T. P. Snutch, J. P. Leonard, M. M. Gilbert, H. A. Lester, N. Davidson, *Proc. Natl. Acad. Sci. U.S.A.* 87, 3391 (1990); T. V. B. Starr, W. Prystay, T. P. Snutch, *ibid.* 88, 5621 (1991).
5. E. Perez-Reyes *et al.*, *J. Biol. Chem.* 267, 1792 (1992).
6. R. Hullin *et al.*, *EMBO J.* 11, 885 (1992).
7. R. W. Tsien, P. T. Ellinor, W. A. Horne, *Trends Pharmacol. Sci.* 12, 349 (1991).
8. M. E. Williams *et al.*, *Neuron* 8, 71 (1992).
9. M. Pragnell, J. Sakamoto, S. D. Jay, K. P. Campbell, *FEBS Lett.* 291, 253 (1991).
10. A. Mikami *et al.*, *Nature* 340, 230 (1989).
11. Y. Mori *et al.*, *ibid.* 350, 398 (1991).
12. T. Aosaki and H. Kasai, *Pfluegers Arch.* 414, 150 (1989).
13. D. Swandulla, E. Carbone, H. D. Lux, *Trends Neurosci.* 14, 46 (1991).
14. E. Sher and F. Clementi, *Neuroscience* 42, 301 (1991).
15. R. Llinás, M. Sugimori, J. W. Lin, B. Cherksey, *Proc. Natl. Acad. Sci. U.S.A.* 86, 1689 (1989); I. M. Mintz *et al.*, *Nature* 355, 827 (1992).
16. S. J. Smith and G. J. Augustine, *Trends Neurosci.* 11, 458 (1988).
17. R. Robitaille, E. M. Adler, M. P. Charlton, *Neuron* 5, 773 (1990); M. W. Cohen, O. T. Jones, K. J. Angelides, *J. Neurosci.* 11, 1032 (1991); F. T. Tarelli, M. Passafaro, F. Clementi, E. Sher, *Brain Res.* 547, 331 (1991).
18. O. T. Jones, D. L. Kunze, K. J. Angelides, *Science* 244, 1189 (1989).
19. E. F. Stanley and G. Goping, *J. Neurosci.* 11, 985 (1991).
20. Recombinant cDNA libraries were prepared, and overlapping α_{1B-1} cDNA clones were isolated from IMR32, human hippocampus, and basal ganglia cDNA libraries and characterized essentially as described (3, 8).
21. We performed PCR analyses as described (8) using IMR32 RNA, human hippocampus RNA, and human genomic DNA with α_{1B-1}-specific primers [nucleotides (nt) 6368 to 6391 and the complement of nt 7071 to 7095] to confirm the α_{1B} termination codon. The RNAs gave the expected 728-bp fragment (α_{1B-1}) as well as a 541-bp
fragment (α_{1B-2}). The genomic DNA product was ~1350 bp. The DNA sequences of α_{1B-1} and α_{1B-2} diverge from each other after nt 6489. The α_{1B-1} subunit contains an additional 187-bp exon that alters the reading frame. After this exon, the α_{1B-1} and α_{1B-2} sequences are identical for the remaining 419 nucleotides characterized from both sequences, α_{1B-1} nt 6677 to 7095 and α_{1B-2} nt 6490 to 6908. The presence of the exon (α_{1B-1}) results in the termination of the coding sequence at nt 7018 to 7020 (TAG); the absence of the exon (α_{1B-2}) results in the termination of the coding sequence at nt 6712 to 6714 (TGA). Differential processing of the α_{1B} primary transcript was confirmed by characterization of the α_{1B} genomic PCR product. An ~270-bp intron was identified between α_{1B-1} nt 6489 and 6490. The α_{1B-1} and α_{1B-2} transcripts result from alternative selection of splice acceptor sites. α_{1B-1} is formed by selection of the splice acceptor at the intron-exon boundary; α_{1B-2} is formed by selection of a splice acceptor identified by an AG dinucleotide at nt 6675 and 6676 of the α_{1B-1} coding sequence.
22. Tissue distribution of the α_{1B-1} and α_{1B-2} transcripts was determined by PCR assays with oligonucleotide primers, nt 6447 to 6470 (Pro^{2149} to Glu^{2157}), and the complement of α_{1B-1}-specific nt 6819 to 6843 (Leu^{2273} to Glu^{2281}). PCR products were probed with an α_{1B-1}-specific oligonucleotide (nt 6513 to 6536; Ser^{2171} to Ala^{2179}) and an α_{1B-2}-specific oligonucleotide (nt 6480 to 6498; Pro^{2160} to Ser^{2166}). The expected size bands were 396 bp (α_{1B-1}) and 209 bp (α_{1B-2}).
23. pcDNAα_{1B-1} was constructed in pcDNA1 (Invitrogen, San Diego, CA) with α1.179 (nt −143 to 2194), α1.177 (nt 2194 to 4160), α1.201 (nt 4160 to 5305), α1.200 (nt 5305 to 6116), and α1.230 (nt 6116 to 7176). DNA sequence analysis revealed that α1.177 has a two-nucleotide deletion (nt 3711 to 3712; Ser^{1237}) that was corrected with a PCR-amplified IMR32 Nar I–Kpn I fragment (nt 3685 to 4160; Gly^{1229} to Gly^{1387}). pHBCaCHα_{2b}(A) and pHBCaCHβ_{2b}.RBS(A), full-length α_{2b} and β_2 constructs in pcDNA1, were described previously (8). HEK293 cells [B. W. Stillman and Y. Gluzman, *Mol. Cell. Biol.* 5, 2051 (1985)] were grown as a monolayer culture in Dulbecco's modified Eagle's medium (Gibco) containing 5% defined-supplemented bovine calf serum (Hyclone) plus penicillin G (100 U/ml) and streptomycin sulfate (100 µg/ml). HEK293 cell transfections were mediated by calcium phosphate [F. M. Ausubel *et al.*, Eds., *Current Protocols in Molecular Biology* (Wiley, New York, 1990), pp. 9.1.1 to 9.1.7]. Cells were transfected (2 x 10⁶ per polylysine-coated plate). Standard transfections (10-cm dish) contained 8 µg of pcDNAα_{1B-1}, 5 µg of pHBCaCHα_{2b}(A), 2 µg of pHBCaCHβ_{2b}.RBS(A), 2 µg of pCMVβ (Clontech β-galactosidase expression plasmid), and pUC18 to maintain a constant mass of 20 µg/ml. Cells were analyzed 48 to 72 hours after transfection. Transfection efficiencies (±10%) were determined by in situ histochemical staining for β-galactosidase activity [J. R. Sanes, J. L. R. Rubenstein, J.-F. Nicolas, *EMBO J.* 5, 3133 (1986)]. Transfection efficiencies generally were >50%.
24. Properties of recombinantly expressed Ca^{2+} channels were studied by whole cell patch-clamp techniques [O. P. Hamill, A. Marty, E. Neher, B. Sakmann, F. J. Sigworth, *Pfluegers Arch.* 391, 85 (1981)]. Recordings were performed on transfected HEK293 cells 2 to 3 days after transfection. Cells were plated at 100,000 to 300,000 cells per polylysine-coated, 35-mm tissue culture dishes (Falcon, Oxnard, CA) 24 hours before recordings. Cells were perfused with 15 mM $BaCl_2$, 125 mM choline chloride, 1 mM $MgCl_2$, and 10 mM Hepes (pH = 7.3) adjusted with tetraethylammonium hydroxide (bath solution). Pipettes were filled with 135 mM CsCl, 10 mM EGTA, 10 mM Hepes, 4 mM Mg–adenosine triphosphate (pH = 7.5) adjusted with tetraethylammonium hydroxide. Sylgard (Dow-Corning, Midland, MI)-coated, fire-polished, and filled pipettes had resistances of 1 to 2 megohm before we established gigohm seals to
cells. ω-CgTx (Bachem), Bay K 8644, and nifedipine (Research Biochemicals, Natick, MA) were prepared as described (8), dissolved in bath solution, and continuously applied by means of puffer pipettes as required for a given experiment. Recordings were performed at room temperature (22° to 25°C). Series resistance compensation (70 to 85%) was employed to minimize voltage error that resulted from pipette access resistance, typically 2 to 3.5 megohm. Current signals were filtered (−3 dB, 4-pole Bessel) at a frequency of 1/4 to 1/5 the sampling rate, which ranged from 0.5 to 3 kHz. Voltage commands were generated, and data were acquired with CLAMPEX (pClamp, Axon Instruments, Foster City, CA). All data shown are corrected for linear leak and capacitive components as described (8). Exponential fitting of currents was performed with CLAMPFIT (Axon).
25. Currents <30 pA were not included because of unreliable measurements. For $\alpha_{1B-1}\alpha_{2b}\beta_2$-transfected cells, currents in 43.6% of the expressing cells ranged from 30 to 200 pA, 43.6% of the cells had currents that ranged from 200 to 1000 pA, and 12.8% had currents that exceeded 1000 pA.
26. We mechanically removed cells from tissue culture plates 48 hours after transfection by spraying with phosphate-buffered saline that contained 0.1% (w/v) bovine serum albumin (BSA). The cells were collected, washed once, and resuspended in assay buffer [10 mM Hepes (pH 7.4), 140 mM NaCl, 5 mM KCl, 12 mM glucose, and BSA (1 mg/ml)]. Specific binding of ^{125}I-ω-CgTx to transfected cells was determined as described (30) with several modifications. Briefly, we performed the assay in 12 mm x 75 mm polypropylene tubes in 0.5 ml of assay buffer by incubating the cells with 100 pM ^{125}I-ω-CgTx (DuPont Biotechnology Systems; 2200 Ci/mmol) for 1 hour at 37°C. Subsequently, 2 ml of ice-cold wash buffer [5 mM Hepes (pH 7.4), 160 mM choline chloride, 1.5 mM $CaCl_2$, and BSA (1 mg/ml)] was added to each tube, and the mixtures were centrifuged at 2300g for 30 min at 4°C. The pellets were washed again and counted for radioactivity. Nonspecific binding was determined in the presence of 20 nM unlabeled ω-CgTx. The optimum cell number was determined by a titration of 1 x 10⁵ to 2 x 10⁶ cells per assay tube. For saturation binding studies, the binding of ^{125}I-ω-CgTx was measured as a function of increasing concentration of ^{125}I-ω-CgTx. Nonspecific binding was subtracted at each concentration. Specific binding was plotted as a function of ^{125}I-ω-CgTx concentration and analyzed by the Scatchard method.
27. M. C. Nowycky, A. P. Fox, R. W. Tsien, *Nature* 316, 440 (1985); A. P. Fox, M. C. Nowycky, R. W. Tsien, *J. Physiol. (London)* 394, 149 (1987).
28. E. Carbone, E. Sher, F. Clementi, *Pfluegers Arch.* 416, 170 (1990).
29. J. A. Wagner, A. M. Snowman, A. Biswas, B. M. Olivera, S. H. Snyder, *J. Neurosci.* 8, 3354 (1988); J. Sakamoto and K. P. Campbell, *J. Biol. Chem.* 266, 18914 (1991); M. K. Ahlijanian, J. Striessnig, W. A. Catterall, *ibid.*, p. 20192; M. W. McEnery, A. M. Snowman, A. H. Sharp, M. E. Adams, S. H. Snyder, *Proc. Natl. Acad. Sci. U.S.A.* 88, 11095 (1991).
30. E. Sher, A. Pandiella, F. Clementi, *FEBS Lett.* 235, 178 (1988).
31. P. Blount, M. M. Smith, J. P. Merlie, *J. Cell Biol.* 111, 2601 (1990).
32. M. R. Plummer, D. E. Logothetis, P. Hess, *Neuron* 2, 1453 (1989); S. W. Jones and T. N. Marks, *J. Gen. Physiol.* 94, 169 (1989).
33. M. R. Plummer and P. Hess, *Nature* 351, 657 (1991).
34. H.-L. Kim, H. Kim, P. Lee, R. G. King, H. Chin, *Proc. Natl. Acad. Sci. U.S.A.* 89, 3251 (1992).
35. The amino acid sequence of a rat α_1 subunit, rbB-I, has been reported [S. J. Dubel *et al.*, *Proc. Natl. Acad. Sci. U.S.A.* 89, 5058 (1992)] and is 92.8% identical to that of the human α_{1B-1} subunit. However, attempts to express the cDNA encoding the rbB-I protein did not yield functional Ca^{2+} channels, thus supporting our conclusion that additional subunits, such as β_2 and α_{2b}, are

required for functional expression.

36. E. Bause, *Biochem. J.* 209, 331 (1983); D. B. Glass, M. R. El-Maghrabi, S. J. Pilkis, *J. Biol. Chem.* 261, 2987 (1986); J. R. Woodgett, K. L. Gould, T. Hunter, *Eur. J. Biochem.* 161, 177 (1986).

37. We thank K. Payne for thoughtful secretarial as-

Membrane Depolarization Induces p140^{trk} and NGF Responsiveness, But Not p75^{LNGFR}, in MAH Cells

Susan J. Birren, Joseph M. Verdi, David J. Anderson*

Nerve growth factor (NGF) is required for the maturation and survival of sympathetic neurons, but the mechanisms controlling expression of the NGF receptor in developing neuroblasts have not been defined. MAH cells, an immortalized sympathoadrenal progenitor cell line, did not respond to NGF and expressed neither low-affinity NGF receptor (p75) nor p140^{trk} messenger RNAs. Depolarizing concentrations of potassium chloride, but none of a variety of growth factors, induced expression of p140^{trk} but not p75 messenger RNA. A functional response to NGF was acquired by MAH cells under these conditions, suggesting that expression of p75 is not essential for this response. Depolarization also permitted a relatively high proportion of MAH cells to develop and survive as neurons in fibroblast growth factor and NGF. These data establish a relation between electrical activity and neurotrophic factor responsiveness in developing neurons, which may operate in the functioning of the mature nervous system as well.

The survival of vertebrate neurons is dependent on neurotrophic factors secreted by their postsynaptic targets. NGF, the prototypic neurotrophic factor, is required for the survival of sympathetic and some sensory neurons (1). The embryonic precursors to sympathetic neurons neither respond to nor require NGF (2–4). This raises the question of how developing sympathetic neuroblasts acquire their responsiveness to and dependence on NGF. We have studied this process with the use of MAH cells a retrovirally immortalized sympathoadrenal progenitor cell line (5). The identification of the product of the proto-oncogene *trk*, p140^{trk} (Trk), as a signal-transducing subunit of the NGF receptor (NGFR) (6, 7) has allowed us to use Trk mRNA expression to assay environmental signals that may induce NGF responsiveness in MAH cells. Here we identify membrane depolarization as one such signal.

MAH cells, like the nonimmortalized progenitors from which they derive, do not undergo neuronal differentiation in response to NGF. The protein p75, the low-affinity NGFR (8, 9), is not expressed by these cells (5). MAH cells grown in the absence of added factors also express little or no Trk mRNA (Fig. 1A, lanes 1 and 2). Thus, the failure of these precursor cells to respond to NGF correlates with their lack

S. J. Birren, Division of Biology, California Institute of Technology, Pasadena, CA 91125.
J. M. Verdi and D. J. Anderson, Division of Biology and the Howard Hughes Medical Institute, California Institute of Technology, Pasadena, CA 91125.

*To whom correspondence should be addressed.

of expression of both types of NGFR mRNAs. We then sought to identify factors that induce expression of NGFR and NGF responsiveness. Previously, we found that basic fibroblast growth factor (bFGF) induced low levels of p75 expression and NGF responsiveness in a small subpopulation of MAH cells (5). However, bFGF failed to induce significant Trk expression in MAH cells, as did a number of other growth and neurotrophic factors (Fig. 1A, lanes 4 through 7, and data not shown). In addition, retinoic acid, which induces high-affinity NGF receptors and NGF dependence in chick sympathetic neuroblasts (10), did not induce Trk mRNA (Fig. 1A, lane 8).

In the chick, depolarization increases the survival of NGF-dependent sympathetic neurons (4). In MAH cells, depolarization stimulated the survival of postmitotic neurons. Depolarization of MAH cells produced by the addition of 40 mM KCl led to an induction of Trk mRNA (Fig. 1A, lane 3). A time course in 40 mM KCl revealed that Trk expression was detectable within 24 hours and reached maximal amounts within 3 days (Fig. 1C, lanes 5 through 8). Reprobing of the same blots with p75 probes revealed that, in contrast to Trk mRNA, p75 mRNA was not induced by 40 mM KCl.

MAH cells require dexamethasone (dex) for long-term survival; when dex is removed, the cells die within 4 to 5 days. In the presence of 5 μM dex, a low steady-state amount of Trk mRNA was detected (Fig. 1B, lane 2). However, even in the

presence of dex an up-regulation of Trk mRNA by 40 mM KCl occurred (Fig. 1B, lane 3), indicating that the effect of depolarization is not simply to maintain the survival of Trk-expressing MAH cells. The time course of Trk induction by 40 mM KCl was similar in the presence of dex (Fig. 1D, lanes 6 through 9) as in its absence, although higher steady-state amounts of Trk mRNA were produced in the presence of dex (compare Fig. 1D, lane 8, with Fig. 1C, lane 7). As was the case in the absence of dex, no induction of p75 mRNA was detected in 40 mM KCl plus dex.

The effect of 40 mM KCl is likely to be produced by membrane depolarization because no induction of Trk mRNA was observed in 40 mM NaCl (Fig. 1, A and B, lanes 9). Moreover, veratridine, an Na$^+$ channel agonist that leads to membrane depolarization, also caused an increase in the amount of Trk mRNA concentrations (data not shown). In PC12 cells, the induction of immediate-early gene expression by membrane depolarization requires the opening of voltage-gated Ca^{2+} channels and depends on extracellular Ca^{2+} (11). Removal of extracellular Ca^{2+} or addition of dihydropyridine antagonists of voltage-gated Ca^{2+} channels resulted in the death of MAH cells within 24 hours, precluding our ability to determine a requirement for Ca^{2+} influx in Trk induction. However, at suboptimal concentrations of KCl (20 mM) (Fig. 1E, lane 4), the Ca^{2+} channel agonist Bay K 8644 potentiated the induction of Trk mRNA (Fig. 1F, lanes 3 and 4), which suggests that Ca^{2+} influx through voltage-gated L-type Ca^{2+} channels is indeed involved in the induction of Trk mRNA by membrane depolarization.

We then sought to determine whether depolarization induces a functional response to NGF. We used two assays of NGF responsiveness: neurite outgrowth and cell number. Cell number reflects both the survival- and proliferation-promoting (12) effects of NGF, although for technical reasons it is difficult to determine the relative contributions of these two processes in this system. NGF responses were assayed after 5 days, by which time most MAH cells had died in control medium (Table 1). Those few cells that survived showed little process outgrowth (Fig. 2A). Similar results were obtained in NGF alone (Fig. 2B and Table 1), indicating that MAH cells do not respond to this factor. Cell number was significantly increased by depolarizing concentrations of KCl (Table 1), although little neurite outgrowth was observed (Fig. 2C). In NGF plus 40 mM KCl, cell number was even higher (Table 1) and the cells bore long neurites (Fig. 2D). These neurite-bearing cells, however, lacked the cell soma hypertrophy characteristic of mature neu-

Structure and Functional Expression of α1, α2, and β Subunits of a Novel Human Neuronal Calcium Channel Subtype

Mark E. Williams, Daniel H. Feldman,
Ann F. McCue, Robert Brenner,*
Gonul Velicelebi, Steven B. Ellis,
and Michael M. Harpold
The Salk Institute Biotechnology/Industrial
Associates, Inc.
505 Coast Boulevard South
La Jolla, California 92037

Summary

The primary structures of human neuronal α_1, α_2, and β subunits of a voltage-dependent Ca^{2+} channel were deduced by characterizing cDNAs. The α_1 subunit (α_{1D}) directs the recombinant expression of a dihydropyridine-sensitive L-type Ca^{2+} channel when coexpressed with the β (β_2) and the α_2 (α_{2b}) subunits in Xenopus oocytes. The recombinant channel is also reversibly blocked by 10–15 μM ω-conotoxin. Expression of the α_{1D} subunit alone, or coexpression with the α_{2b} subunit, did not elicit functional Ca^{2+} channel activity. Thus, the β_2 subunit appears to serve an obligatory function, whereas the α_{2b} subunit appears to play an accessory role that potentiates expression of the channel. The primary transcripts encoding the α_{1D}, α_2, and β subunits are differentially processed. At least two forms of neuronal α_{1D} were identified. Different forms of α_2 and β transcripts were also identified in CNS, skeletal muscle, and aorta tissues.

Introduction

The primary pathway by which Ca^{2+} enters excitable cells is through voltage-dependent Ca^{2+} channels present in cellular membranes (Bean, 1989). Multiple subtypes of these channels have been identified (Hess, 1990), the best characterized of which is the rabbit skeletal muscle dihydropyridine (DHP)-sensitive Ca^{2+} channel, consisting of four tightly coupled subunits, α_1, α_2, β, and γ (Campbell et al., 1988). Each of these subunits has been characterized by cDNA cloning (Tanabe et al., 1987; Ellis et al., 1988; Ruth et al., 1989; Jay et al., 1990). Recent evidence suggests that different α_1 subunits are encoded by a gene family comprising at least five distinct genes, some of which are expressed in several tissues (Ellis et al., 1988; Mikami et al., 1989; Perez-Reyes et al., 1990; Snutch et al., 1990). The gene encoding the α_1 subunit expressed in rabbit skeletal muscle directs the recombinant expression of a functional DHP-sensitive Ca^{2+} channel in cultured myotubes of mdg mice and in mouse L cells (Tanabe et al., 1988; Perez-Reyes et al., 1989). A second gene, encoding α_1 subunits expressed in rabbit cardiac and lung tissues, directs the synthesis of

DHP-sensitive Ca^{2+} channels in Xenopus oocytes (Mikami et al., 1989; Biel et al., 1990). In contrast, a third α_1 subunit gene, expressed in rabbit brain, directs the synthesis of Ca^{2+} channels that are insensitive to both DHPs and ω-conotoxin GVIA (ω-CgTx) when coexpressed with the rabbit skeletal muscle α_2 and β subunits in Xenopus oocytes (Mori et al., 1991). These expression studies in oocytes demonstrated that the α_1 subunit forms the pore through which Ca^{2+} enters the cell. The functional expression of α_1 subunits encoded by the two remaining genes has not yet been reported.

The entry of Ca^{2+} through voltage-dependent Ca^{2+} channels in neurons controls diverse functions, such as neurotransmitter release, excitability, and differentiation (Tsien et al., 1988). On the basis of biophysical and pharmacological characterizations, four subtypes of neuronal voltage-dependent Ca^{2+} channels have been proposed (Llinás et al., 1989; Swandulla et al., 1991). Although specific neuronal functions have been ascribed to different Ca^{2+} channel subtypes, the analysis has been difficult due to the coexistence of multiple subtypes in individual cells (Miller, 1987; Bean, 1989; Hess, 1990; Swandulla et al., 1991). One important step in defining subtype–function relationships is the cloning and expression of each neuronal subtype as a pure population. We report the complete amino acid sequence and functional expression of three subunits of a human neuronal L-type voltage-dependent Ca^{2+} channel: an α_1 subunit (designated α_{1D}), an α_2 subunit (designated α_{2b}), and a β subunit (designated β_2). A description of the nomenclature used to designate the different Ca^{2+} channel subunits is provided in the Experimental Procedures. We also report tissue-specific processing of the α_2 and β transcripts.

Results

Cloning and Characterization of Three Human Neuronal Voltage-Dependent Ca^{2+} Channel Subunits

We previously reported the isolation of cDNAs that encode the α_1, α_2, β, and γ subunits of the rabbit skeletal muscle DHP-sensitive, L-type Ca^{2+} channel (Ellis et al., 1988; Jay et al., 1990). These subunit cDNAs were used as probes to isolate related human neuronal cDNAs as described in the Experimental Procedures. The primary structures of the human neuronal α_{1D}, α_{2b}, and β_2 subunits (Figure 1; see Figure 3 and Figure 4) were deduced from these cDNA sequences.

α_{1D} Subunit

The primary structure of the human α_{1D} subunit (Figure 1) comprises 2161 amino acids, yielding a calculated molecular weight of 245,163. The α_{1D} sequence is most similar (96.3% deduced amino acid sequence identity) to the previously reported 188 amino acid

*Present address: Department of Zoology, University of Texas, Austin, Texas 78712.

Figure 1. α₁D Nucleotide and Deduced Amino Acid Sequences

The 5' untranslated sequence is negatively numbered. Positive numbering begins at the first nucleotide of the proposed initiating codon. The number of the nucleotide and amino acid residue is given at the end of each line. The proposed transmembrane segments S1–S6 in each of the repeats I–IV are shown (brackets).

partial rat brain class D cDNA (Snutch et al., 1990). The translation initiation site was assigned to the first methionine codon that appears downstream of an in-frame nonsense codon. Interestingly, 7 methionine codons appear at the beginning of the putative coding sequence, followed by 2 lysine codons and an eighth methionine codon; none of these methionine codons are contained within the consensus sequence for eu-caryotic initiation codons (Kozak, 1987). This series of methionine codons was confirmed by direct se-quence analysis of cloned polymerase chain reaction (PCR) products derived from reactions performed on human neuroblastoma IMR32 cell cytoplasmic RNA, as described in the Experimental Procedures.

The predicted structure of the α_{1D} subunit consists of four repeating domains, each domain comprised of five hydrophobic segments (S1, S2, S3, S5, and S6) and one positively charged segment (S4), suggesting the same transmembrane topology as described pre-viously for Ca^{2+} channel α_1 subunits and Na^+ channels (Numa and Noda, 1986; Tanabe et al., 1987; Mikami et al., 1989; Biel et al., 1990; Koch et al., 1990; Mori et al., 1991). Based on this proposed topology, the α_{1D} subunit has 3 of 12 potential N-glycosylation sites (Bause, 1983) assigned to the extracellular side and nine of ten potential cAMP–dependent phosphoryla-tion sites (Glass et al., 1986) and 22 of 26 potential protein kinase C phosphorylation sites (Woodgett et al., 1986) assigned to the cytoplasmic side of the cellu-lar membrane (Figure 2).

The α_{1D} cDNA clone α1.136 was found to encode an incompletely processed transcript containing two exons encoding the IS6 transmembrane domain, des-ignated α_{1D} exon A and α_{1D} exon B. The deduced amino acid sequences are MNDAMGFELPWVYFVSL-VIFGSFFVLNLVLGVLSG and VNDAIGWEWPWVYFV-SLIILGSFFVLNLVLGVLSG, respectively, which share 83% identity. Exon A was present in clone α1.144, which was used for the construction of the full-length α_{1D} cDNA used in the present study (Figure 1).

The deduced amino acid sequences of two different α_1 subunits, the rabbit cardiac (Mikami et al., 1989) and the rabbit brain BI-2 (Mori et al. 1991), previously expressed in Xenopus oocytes, are shown aligned with the human α_{1D} sequence (Figure 2). The amino acid sequence identity of α_{1D} to these sequences is significant: 70.3% and 40.5% for the cardiac and BI-2 sequences, respectively. The sequence identity is well conserved through the four repeating domains, 79.7% and 50.5% for the α_{1D}–cardiac and the α_{1D}–BI-2 pairs, respectively. Most noteworthy is the divergence of the α_{1D} and cardiac sequences compared with the BI-2 sequence through the putative DHP-binding region (Regulla et al., 1991). In this region, the α_{1D} and cardiac DHP-sensitive forms differ by a single amino acid (Ser-1490) as does the rabbit skeletal muscle sequence (Ala-1404), whereas the BI-2 DHP-insensitive form has 18 amino acid substitutions in this region (Figure 2). This evidence, together with the results of the expres-sion studies reported here (see below), supports the proposed identity of the DHP-binding region.

α_{2b} Subunit

The primary structure of the human brain α_{2b} subunit (Figure 3) consists of 1091 amino acids, yielding a cal-culated molecular weight of 123,182. The amino acid sequence homology is 97.1% identical to the rabbit skeletal muscle α_{2a} subunit sequence (Figure 3) and has essentially an identical predicted topography and secondary structure (Ellis et al., 1988; Jay et al., 1991), with the exceptions of a 19 amino acid deletion in the human sequence compared with the rabbit sequence (α_{2a} residues Pro-507 to Gln-525) and a 7 amino acid insertion in the human sequence compared with the rabbit sequence (α_{2b} residues Lys-602 to Asp-608). The 16 potential glycosylation sites that were identified in the rabbit skeletal muscle α_{2a} subunit (Jay et al., 1991) also are conserved in the human α_{2b} sequence. Previ-ous studies suggest that posttranslational processing of the rabbit skeletal α_{2a} subunit results in a heteroge-neous population of δ peptides, all of which begin at Ala-935 (Jay et al., 1991). The human brain α_{2b} sequence has two conservative amino acid substitutions at this proposed cleavage site, Val-923 and Glu-924 replacing Ala-935 and Asp-936, respectively (Figure 3).

β_2 and β_3 Subunits

The primary structure of the human brain β_2 subunit (Figure 4) comprises 478 amino acids and has a calcu-lated molecular weight of 52,934. The amino acid se-quence homology is 96.9% identical to the rabbit skel-etal muscle β_1 subunit sequence (Figure 4). The β_2 subunit has essentially an identical topography and secondary structure as predicted for the rabbit skele-tal muscle β_1 subunit (Ruth et al., 1989) except that the deduced human β_2 sequence has a deletion of 45 amino acids (Ala-217 to Lys-261). The lack of this region in β_2 removes the second α helical domain proposed for the rabbit skeletal muscle β_1 subunit (Ruth et al., 1989). Thirteen of sixteen potential phosphorylation sites identified in the rabbit skeletal muscle β_1 subunit (Ruth et al., 1989) are conserved in the human β_2 se-quence (Figure 4). Two sites are changed due to amino acid substitutions (β_1 Ser-179 and Ser-182), and the third is removed by the 45 amino acid deletion (β_1 Ser-238).

Another form of β, designated β_3, which has the same deduced 45 amino acid deletion, was identified in the hippocampus cDNA library. Clone $\lambda\beta$4 encodes the β_3 cDNA and diverges from β_2 after nucleotide 1332. The β_3 cDNA extends another 429 nucleotides with no translation stop codon identified (data not shown). A GT splice donor is not present at the point of divergence between the β_2 and β_3 sequences. A complete characterization of β_3 is in progress.

Tissue-Specific Processing of the α_2 and β Transcripts and Distribution of α_{1D}, α_2, and β mRNAs

PCR analysis and hybridization with oligonucleotides derived from α_{2a}– or α_{2b}–specific regions (the 19 amino acid region or the 7 amino acid region, respec-tively; Figure 3) demonstrated that the human skeletal

Figure 2. Alignment of Deduced Amino Acid Sequences of α₁ Subunits

The amino acid sequences of the human neuronal Ca^{2+} channel α_{1D} (Hum 1D), the rabbit cardiac α_1 (Card; Mikami et al., 1989), and the rabbit brain α_1 (BI-2; Mori et al., 1991) are shown in single-letter code. The numbering begins with the proposed initiating methionine. The number of the amino acid residue at the end of each line is given. Identical residues at one position in two of the three sequences are shown as white letters on black background. The putative transmembrane segments S1–S6 in each of the repeats I–IV are shown (brackets). The putative DHP-binding regions (N1, N2, A2; Regulla et al., 1991) are shown (underlined). Potential N-glycosylation (o), cAMP-dependent phosphorylation (<), and protein kinase C phosphorylation (▷) sites are shown. Potential targets of either kinase are labeled (+).

Figure 3. Determined cDNA Sequence of α₁ₛ and Alignment of the Deduced Amino Acid Sequence with the Deduced Rabbit Skeletal Muscle α₂ₛ Sequence

For the rabbit α₂ₛ sequence (Rab; Ellis et al., 1988), only the amino acid differences compared with the human α₁ₛ sequence (Hum) are shown. The 5' untranslated sequence is negatively numbered. Positive numbering begins at the first nucleotide of the proposed initiating codon. The number of the nucleotide and amino acid residue is given at the end of each line. Negative numbers for amino acids designate residues contained in the proposed signal sequence (Ellis et al., 1988) beginning with the initiating methionine (−24 and −26). The positive numbering begins at the NH₂–terminal residue (glutamic acid) of the mature protein. Amino acid sequence differences and insertions/deletions are identified by the black boxes. Potential N-glycosylation (◊), cAMP–dependent phosphorylation (◁), and protein kinase C phosphorylation (▷) sites are shown. The potential target of either kinase is labeled (+).

muscle α_2 transcript is processed in a manner similar to the rabbit skeletal muscle transcript (540 bp bands; Figure 5A). Furthermore, the α_2 transcripts expressed in IMR32 cells and human CNS tissues (501 bp bands; Figure 5B) and the α_2 transcript expressed in aorta tissue (490 bp band; Figure 5B) are processed differentially to yield at least two additional α_2 transcript species, α_{2b} (Figure 3) and α_{2c}, respectively.

PCR analysis of β-specific RNAs showed that the β primary transcript is also processed in a tissue-specific manner. Analysis of human skeletal muscle RNA detected the 135 nucleotides absent in β_2 (Figure 4) and, thus, confirmed the presence of a distinct skeletal muscle β_1 transcript (Figure 5C). In addition to the β_1 form expressed in skeletal muscle and the β_2 and β_3 forms expressed in the CNS, another form, designated β_4, was detected in aorta tissue having a 156 nucleotide deletion relative to the skeletal muscle β_1 transcript (Figure 5C).

To confirm the tissue-specific processing of the β subunit primary transcript, β-specific PCR products of human skeletal muscle and aorta were cloned, and the DNA sequence was determined. The deduced human skeletal muscle amino acid sequence is 92% identical to the rabbit skeletal muscle sequence from position Gly-210 to Lys-261 (Figure 4). The β_2 sequence has a proposed alternative exon (Ala-210 to Ser-216) that

probably corresponds to either the human skeletal muscle sequence Gly-210 to Leu-216 (GNEMTNL) or Arg-255 to Lys-261 (RIPFFKK). The deduced aorta sequence lacks the region between residues Ser-209 and Thr-217 (Figure 4).

PCR analysis performed on RNAs isolated from several human primary tissues and IMR32 cells identified an α_{1D} transcript in IMR32 cells and each of the human CNS tissues, but not in human skeletal muscle (Figure 5D). An α_2 transcript was detected in all RNAs analyzed (Figures 5A and 5B), as was a β transcript (Figure 5C).

Functional Expression in Xenopus Oocytes

The expression of the human neuronal α_{1D}, α_{2b}, and β_2 subunits was studied in Xenopus oocytes. mRNAs encoding each subunit were synthesized in vitro and were injected into oocytes either alone or in various combinations. The oocytes then were examined for inward Ba^{2+} currents (I_{Ba}) mediated by voltage-dependent Ca^{2+} channels.
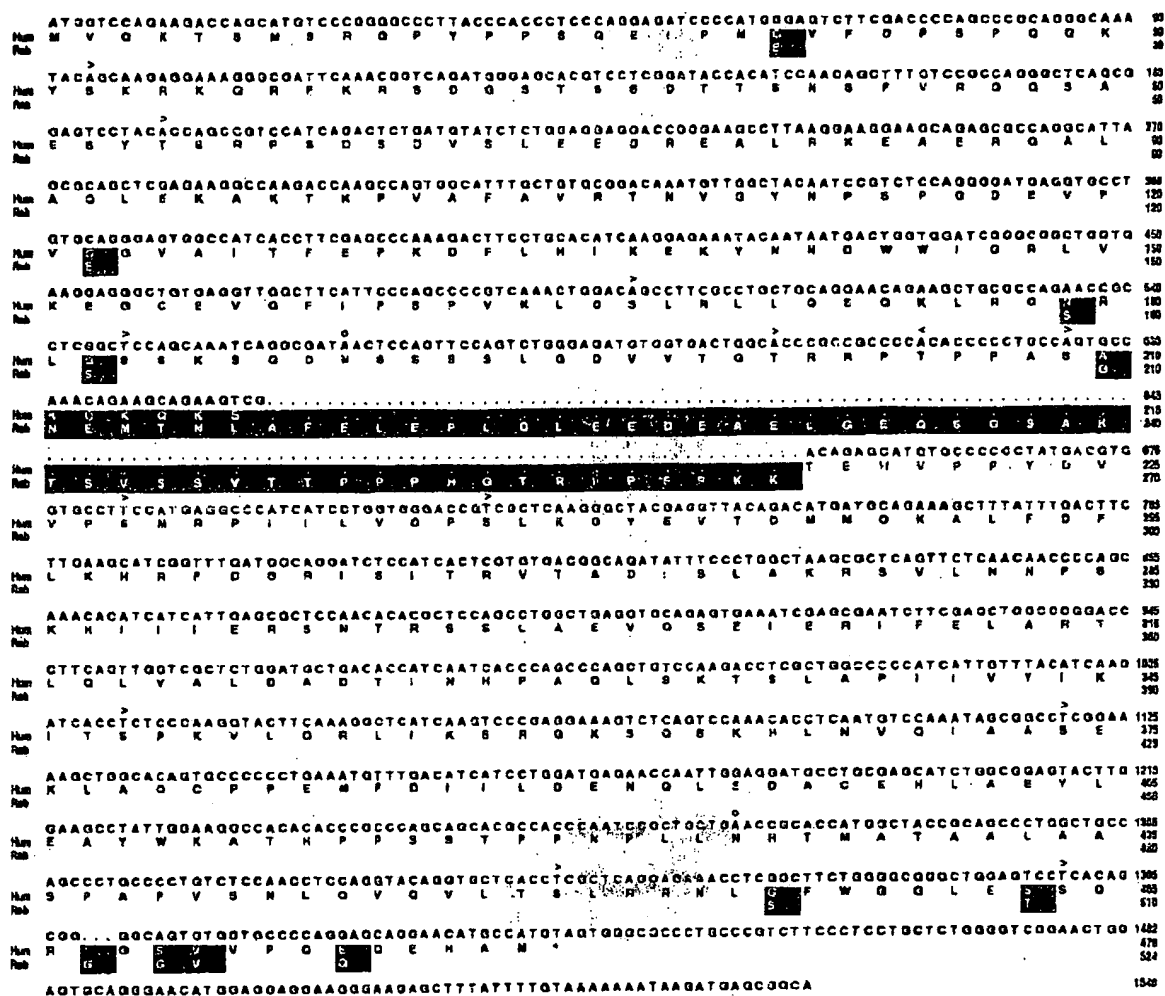
Oocytes coinjected with the α_{1D}, α_{2b}, and β_2 mRNAs expressed sustained I_{Ba} upon depolarization (162 ± 121 nA, n = 46) that typically showed little inactivation during test pulses ranging from 140–700 ms (Figure 6A). A series of voltage steps revealed currents that appeared at approximately −30 mV and peaked at approximately 0 mV (Figure 6B). Application of the DHP

[Figure 4: DNA and deduced amino acid sequence alignment]

Figure 4. Determined cDNA Sequence of β_2 and Alignment of the Deduced Amino Acid Sequence with the Deduced Rabbit Skeletal Muscle β_1 Sequence

For the rabbit β_1 sequence (Rab; Ruth et al., 1989), only the amino acid differences compared with the human β_2 sequence (Hum) are shown. See legend of Figure 3 for description of symbols and numbering.

Ca^{2+} channel agonist Bay K 8644 increased the magnitude of the $\alpha_{1D}\alpha_{2b}\beta_2$-mediated currents, prolonged the "tail" currents present upon repolarization of the cell, and induced a hyperpolarizing shift in current activation (Figures 6A and 6B). Application of the DHP Ca^{2+} channel antagonist nifedipine blocked a substantial fraction of the I_{Ba} in oocytes coinjected with α_{1D}, α_{2b}, and β_2 (91% ± 6%, n = 7; Figure 6C). Much of the I_{Ba} recovered when the holding potential was shifted from −50 mV to −90 mV (data not shown), consistent with the voltage-dependent block by nifedipine (Bean, 1984; Sanguinetti and Kass, 1984). A residual inactivating component of I_{Ba} typically remained after nifedipine application. Consistent with previous studies on neuronal L-type Ca^{2+} channels (Fox et al., 1987), the $\alpha_{1D}\alpha_{2b}\beta_2$-mediated I_{Ba} was blocked completely by 50 μM Cd^{2+}, but only approximately 15% by 100 μM Ni^{2+}.

The $\alpha_{1D}\alpha_{2b}\beta_2$-mediated I_{Ba} was blocked weakly (54% ± 29%, n = 7) and reversibly by relatively high concentrations (10–15 μM) of ω-CgTx (Figure 6D). Bay K 8644 was first applied to the cell in order to determine the effect of ω-CgTx on the DHP-sensitive current component that was distinguished by the prolonged tail currents. Both the test currents and the accompanying tail currents were blocked progressively within 1–3 min after application of ω-CgTx, but both recovered partially as the ω-CgTx was flushed from the bath.

The contribution of the α_{2b} and β_2 subunits to the $\alpha_{1D}\alpha_{2b}\beta_2$-mediated current was assayed by expression of the α_{1D} subunit alone or in combination with either the β_2 subunit or the α_{2b} subunit. Oocytes injected with only the α_{1D} mRNA produced no discernable I_{Ba} upon depolarization (n = 10). Oocytes coinjected with the α_{1D} and β_2 mRNAs expressed I_{Ba} (105 ± 39 nA, n = 4) that resembled the $\alpha_{1D}\alpha_{2b}\beta_2$-mediated currents,
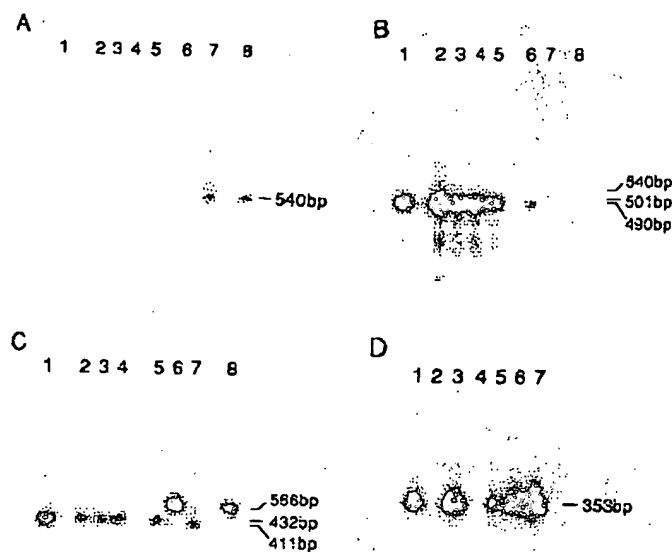
Figure 5. Autoradiographs of PCR Products Showing Distribution of Voltage-Dependent Ca²⁺ Channel Subunit Transcripts and Alternative Splicing of the α_2 and β Transcripts

IMR32 cytoplasmic RNA and human primary tissue poly(A)⁺ RNAs were used as templates to synthesize cDNA prior to PCR analysis.

(A and B) PCR products of pHBCaCHα₃+, a human brain α_{2b} cDNA clone (lane 1), IMR32 cells (lane 2), hippocampus and basal ganglia (lane 3), habenula (lane 4), thalamus (lane 5), aorta (lane 6), skeletal muscle (lane 7), and pα2.15Δ5′, a rabbit skeletal muscle α_2 clone (lane 8), were hybridized with (A) an α_2 oligonucleotide (nucleotides 1597–1619 corresponding to Pro-507 to Thr-514; Ellis et al., 1988) or (B) an α_{2b} oligonucleotide (nucleotides 1876–1896 corresponding to Lys-602 to Asp-608). The PCR reactions were primed with human α_{2b} oligonucleotides, nucleotides 1455–1479, and the complement of nucleotides 1931–1955. An approximately equal mass of DNA was present in each lane. The sizes of the 490 bp, 501 bp, and 540 bp α_2-specific PCR products derived from human aorta, IMR32 cell and CNS tissues, and skeletal muscle RNAs, respectively, were further

confirmed by electrophoresis through a 1% agarose/2% NuSieve composite gel. The weaker hybridization of the human α_{2b}–derived oligonucleotide with the 490 bp aorta and 540 bp skeletal muscle PCR products further supports their difference from the α_{2b} transcript. Each band observed also hybridized with an α_2 tissue nonspecific probe, nucleotides 1601–1626 (data not shown).

(C) PCR products of pHBCaCHβ1, a human brain β_2 cDNA clone (lane 1), IMR32 cells (lane 2), hippocampus and basal ganglia (lane 3), habenula (lane 4), thalamus (lane 5), skeletal muscle (lane 6), aorta (lane 7), and pRSKmCaCHβ2, a rabbit skeletal muscle β_1 cDNA clone (lane 8), were hybridized with a β_2 oligonucleotide, nucleotides 755–784. The PCR products were primed with β_2 oligonucleotides, nucleotides 541–560, and the complement of nucleotides 953–972.

(D) PCR products of pVDCCIII(A), an α_{1b} cDNA clone (lane 1), human genomic DNA (lane 2), IMR32 cells (lane 3), skeletal muscle (lane 4), hippocampus and basal ganglia (lane 5), habenula (lane 6), and thalamus (lane 7), were hybridized with an α_{1b} oligonucleotide, nucleotides 164–187. The PCR products were primed with α_{1b} oligonucleotides, nucleotides −39 to −18, and the complement of nucleotides 201–314.
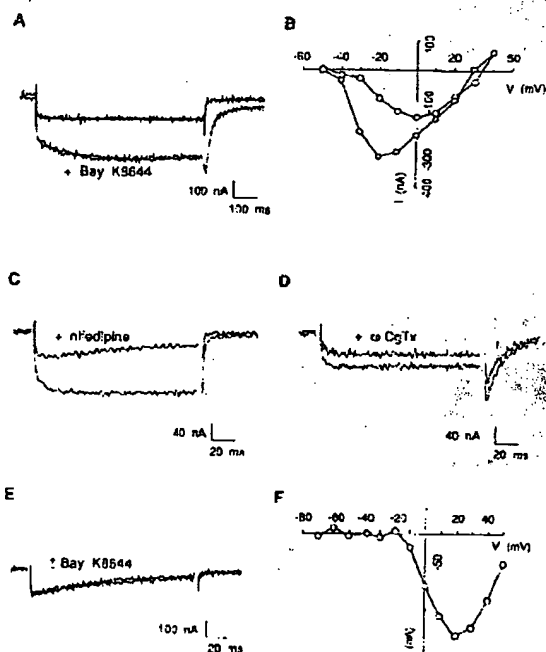

Figure 6. Functional Expression of α_{1D}, α_{2b}, and β_2 in Xenopus Oocytes

(A) I_{Ba} recorded before and after application of Bay K 8644 (1 μM) in an oocyte injected with α_{1D}, α_{2b}, and β_2 mRNAs. Test pulse, −10 mV; holding potential, −50 mV.

(B) Peak current–voltage relations before (open circles) and after (closed circles) application of Bay K 8644 for the α_{1D}, α_{2b}, and β_2 mRNA-injected cell of (A). Holding potential, −50 mV.

(C) Currents before and after (+) application of nifedipine (5 μM) in an oocyte injected with α_{1D}, α_{2b}, and β_2 mRNAs. Current traces are signal averages of three traces before and three traces after application of nifedipine. Test pulse, 0 mV; holding potential, −50 mV.

(D) Currents in the absence and presence (+) of ω-CgTx (10 uM) in an oocyte injected with α_{1D}, α_{2b}, and β_2 mRNAs. Bay K 8644 (1 μM) was present throughout. Current traces are signal averages of three traces before and three traces after application of ω-CgTx for approximately 1.5 min. Test pulse, 0 mV; holding potential, −50 mV.

(E) Currents before and after application of Bay K 8644 (1 μM) in an oocyte injected with α_{2b} and β_2 mRNAs. Superimposed current traces are signal averages of four traces before and four traces after application of Bay K 8644. Test pulse, 20 mV; holding potential, −90 mV.

(F) Peak current–voltage relation for the α_{2b} and β_2 mRNA-injected cell of (E). Holding potential, −90 mV.

although the magnitude of the current was, on average, smaller. Two of four oocytes injected with $\alpha_{1D}\beta_2$ responded to Bay K 8644 application similarly to the $\alpha_{1D}\alpha_{2b}\beta_2$-mediated currents, whereas the remaining two showed no response. Three of five oocytes coinjected with the α_{1D} and α_{2b} mRNAs displayed very small currents (15–30 nA) and were unresponsive to Bay K 8644.

To ensure that the currents observed in the $\alpha_{1D}\alpha_{2b}$-β_2-injected oocytes were mediated by the α_{1D} subunit, expression of the β_2 or α_{2b} subunits alone or both together was assayed. Oocytes injected with the α_{2b} mRNA displayed no detectable I_{Ba} ($n = 5$). Surprisingly, oocytes injected with β_2 mRNA displayed I_{Ba} upon depolarization (54 ± 23 nA, $n = 5$), and $\alpha_{2b}\beta_2$-injected oocytes displayed I_{Ba} (Figure 6E) approximately 50% larger than the I_{Ba} of β_2-injected oocytes (81 ± 60 nA, $n = 21$). Oocytes injected with the β_2 mRNA or the α_{2b} and β_2 mRNAs together displayed I_{Ba} that typically was observed first at -30 mV and that peaked at 10–20 mV (Figure 6F). Macroscopically, the β_2- and $\alpha_{2b}\beta_2$-induced currents were indistinguishable.

In contrast to the $\alpha_{1D}\alpha_{2b}\beta_2$-mediated currents, the β_2 and $\alpha_{2b}\beta_2$ currents showed both a significant inactivation during the test pulse and a strong sensitivity to the holding potential. The I_{Ba} observed in oocytes coinjected with α_{2b} and β_2 mRNAs usually inactivated markedly during a 140 ms pulse (Figure 6E). Changing the holding potential of oocytes coinjected with the α_{2b} and β_2 mRNAs from -90 mV to -50 mV reduced the I_{Ba} 81% $\pm$ 15% ($n = 11$). In contrast, I_{Ba} measured in oocytes coinjected with the $\alpha_{1D}\alpha_{2b}\beta_1$ mRNAs was reduced 24% $\pm$ 16% ($n = 11$) when the holding potential was changed from -90 mV to -50 mV.

The $\alpha_{2b}\beta_2$-mediated I_{Ba} was also pharmacologically distinct from the $\alpha_{1D}\alpha_{2b}\beta_2$-mediated current. Oocytes coinjected with α_{2b} and β_2 mRNAs displayed I_{Ba} that was insensitive to Bay K 8644 ($n = 11$; Figure 6E). Nifedipine sensitivity was difficult to measure because of the holding potential sensitivity of both nifedipine and the $\alpha_{2b}\beta_2$-mediated I_{Ba}. Nevertheless, two oocytes coinjected with the α_{2b} and β_2 mRNAs displayed measurable I_{Ba} (25–45 nA) when depolarized from a holding potential of -50 mV, and these currents were insensitive to nifedipine (5–10 μM) application. The $\alpha_{2b}\beta_2$-mediated I_{Ba} showed a sensitivity to heavy metals similar to the $\alpha_{1D}\alpha_{2b}\beta_2$-mediated current.

Discussion

Distinct Neuronal Ca²⁺ Channel Subunits Comprise a Novel DHP-Sensitive Subtype

Our results demonstrate that the α_{1D} subunit mediates DHP-sensitive, high voltage–activated, long-lasting Ca²⁺ channel activity (Figure 6A). Significant functional expression in oocytes of the α_{1D} subunit is dependent on the coexpression of the β_2 subunit and is enhanced by coexpression with the α_{2b} subunit. The biophysical properties of activation and inactivation kinetics and voltage sensitivity of the channel formed

by the α_{1D}, α_{2b}, and β_2 subunits are generally consistent with previous characterizations of neuronal L-type Ca²⁺ channels (Bean, 1989; Hess, 1990; Swandulla et al., 1991).

Immunoprecipitation of a neuronal DHP receptor previously has revealed the presence of an α_1, α_2, and β subunit complex (Ahlijanian et al., 1990). As an initial step toward a detailed characterization of the multiple subtypes of neuronal voltage-dependent Ca²⁺ channels, we cloned and expressed the human neuronal α_{1D}, α_{2b}, and β_2 subunits. Characterization of these clones revealed that both the α_{1D} and β transcripts expressed in neuronal tissue are differentially processed. Alternatively spliced α_{1D} transcripts involve at least four regions: the IS6 region reported here, the cytoplasmic loop between IS6 and IIS1 (Hui et al., 1991; data not shown), the IVS3 region, and the extracellular loop between the IVS3 and IVS4 regions (Perez-Reyes et al., 1990). In addition, a recent report described a possible form of α_{1D} with a truncated carboxyl terminus, although the functional significance of this form is unknown (Hui et al., 1991). Minimally, three forms of the α_2 subunit exist (Figures 5A and 5B): α_{2a}, expressed in skeletal muscle (Ellis et al., 1988); α_{2b}, expressed in neuronal tissues; and α_{2c}, expressed in aorta. At least four forms of the β subunit also exist: β_1, expressed in skeletal muscle; β_2 and β_3, expressed in human brain tissue; and β_4, detected in aorta (Figure 5C). Additional forms of the β subunit may also be expressed, as indicated by two β-specific transcripts identified in skeletal muscle (Ruth et al., 1989).

Recently, a rabbit brain α_1 subunit, designated BI, was cloned and expressed (Mori et al., 1991). Not only does this subunit differ structurally from the α_{1D} subunit (Figure 2), but the biophysical and pharmacological properties of the Ca²⁺ channel, formed by coexpression of the BI subunit with the rabbit skeletal muscle α_{2a} and β_1 subunits, differ from those of the human neuronal $\alpha_{1D}\alpha_{2b}\beta_2$ recombinant channel. The BI-mediated Ca²⁺ channel activity is insensitive to both DHPs and ω-CgTx and inactivates rapidly compared with the α_{1D}-mediated activity. The expression in Xenopus oocytes of both the BI-mediated and α_{1D}-mediated I_{Ba} requires the coexpression of a β subunit. Thus, two structurally and pharmacologically distinct α_1 subunits expressed in neuronal tissues require a β subunit for functional Ca²⁺ channel activity in oocytes, in contrast to the α_1 subunits expressed in cardiac (Mikami et al., 1989) and smooth muscle (Biel et al., 1990).

The α_1 subunits expressed in both cardiac and lung tissues are likely encoded by the same gene (Biel et al., 1990). This gene encodes mRNAs that direct the synthesis of DHP-sensitive Ca²⁺ channels in Xenopus oocytes with macroscopic biophysical properties similar to the $\alpha_{1D}\alpha_{2b}\beta_2$ channel (Mikami et al., 1989; Biel et al., 1990). However, the human neuronal $\alpha_{1D}\alpha_{2b}\beta_2$ DHP-sensitive channel has a current–voltage relation that is shifted by approximately -20 mV, and its tail currents are markedly prolonged after Bay K 8644 application compared with the cardiac and lung channel

types. A comparison of the single-channel properties might further distinguish these different DHP-sensitive L-type Ca^{2+} channels.

The β_2 Subunit Stimulates DHP-Insensitive I_{Ba} in Xenopus Oocytes

Our results suggest that the α_2 and β subunits expressed in skeletal muscle (α_{2a} and β_1) differ structurally (Figure 3; Figure 4; Figure 5) and possibly functionally from the α_2 and β subunits expressed in brain tissue (α_{2b} and β_2). Xenopus oocytes coinjected with the rabbit skeletal muscle α_{2a} and β_1 mRNAs apparently do not display I_{Ba} upon depolarization (Mori et al., 1991). This is in contrast to our observation that oocytes injected with the human neuronal β_2 mRNA alone or coinjected with the β_2 and α_{2b} mRNAs display significant I_{Ba} upon depolarization. Coexpression of the α_{2b} subunit enhances the I_{Ba}, but α_{2b} mRNA shows no activity when injected alone.

The Ca^{2+} channel expressed in $\alpha_{2b}\beta_2$-injected oocytes has pharmacological and biophysical properties that resemble Xenopus oocyte endogenous voltage-dependent Ca^{2+} channels (Dascal et al., 1986). Similar to the skeletal muscle β_1 subunit (Ruth et al., 1989), the β_2 subunit lacks hydrophobic segments capable of forming transmembrane domains. Thus, it is unlikely that the β_2 subunit alone is forming an ion channel. It is more probable that a homologous α_1 subunit exists in oocytes comprising an endogenous Ca^{2+} channel and that the activity mediated by this α_1 subunit is enhanced by the expression of the β_2 subunit, similar to that observed for the α_{1D} and BI activities. Further information concerning the structure of the endogenous Xenopus oocyte Ca^{2+} channel is not yet available.

The Ca^{2+} channel stimulated by the presence of the β_2 subunit may contribute an inactivating, DHP-insensitive component of I_{Ba} to the total current in $\alpha_{1D}\alpha_{2b}\beta_2$-injected oocytes, especially when recorded from strongly negative holding potentials. Recordings made from $\alpha_{1D}\alpha_{2b}\beta_2$-injected oocytes at different holding potentials support this possibility and indicate that such contamination can be reduced, though not necessarily eliminated, by holding at −50 mV. The DHP-insensitive β_2-mediated current may account for the residual inactivating I_{Ba} detected in $\alpha_{1D}\alpha_{2b}\beta_2$-injected oocytes in the presence of nifedipine (Figure 6C).

ω-CgTx Interacts with the Neuronal DHP-Sensitive Ca^{2+} Channel

ω-CgTx blocks neuronal N-type Ca^{2+} channels irreversibly (Feldman et al., 1987; McCleskey et al., 1987). In contrast to this high affinity block, ω-CgTx blocks the $\alpha_{1D}\alpha_{2b}\beta_2$ channel reversibly with an affinity probably in the micromolar range, as indicated by the partial block with 10–15 μM ω-CgTx. Although preliminary experiments indicate that the $\alpha_{2b}\beta_2$-mediated channel may be inhibited by ω-CgTx, block of Bay K 8644-induced tail currents in $\alpha_{1D}\alpha_{2b}\beta_2$-injected oocytes demonstrates that ω-CgTx also interacts with the

DHP-sensitive $\alpha_{1D}\alpha_{2b}\beta_2$ channel. Reversible block by ω-CgTx of L-type (Aosaki and Kasai, 1989), T-type (McCleskey et al., 1987), and a subclass of N-type (Plummer et al., 1989) Ca^{2+} channels has been reported. Furthermore, Ca^{2+}-dependent ATP release from elasmobranch electroplax synaptosomes is blocked reversibly by ω-CgTx with micromolar affinity (Yeager et al., 1987). It thus appears that variable affinity for ω-CgTx may be shared by several types of voltage-dependent Ca^{2+} channels. A weak block such as we have demonstrated for the $\alpha_{1D}\alpha_{2b}\beta_2$ L-type channel may account for the conflicting results reported in the literature concerning the ability of ω-CgTx to block neuronal L-type channels (McCleskey et al., 1987; Suzuki and Yoshioka, 1987; Aosaki and Kasai, 1989; Plummer et al., 1989).

Conclusion

The function of DHP-sensitive Ca^{2+} channels in skeletal and cardiac muscle has been extensively studied (Hess, 1990). In contrast, the role of the neuronal L-type Ca^{2+} channel is poorly understood (Miller, 1987). L-type Ca^{2+} channels may mediate the release of neurotransmitters from some types of neurons (Holz et al., 1988). However, functional analysis is difficult due to the mixed population of voltage-dependent Ca^{2+} channel subtypes in continuous cell lines as well as cells in primary tissues. For example, L-type Ca^{2+} channels contribute a minor fraction of the I_{Ba} detectable in the cell bodies of IMR32 cells (Carbone et al., 1990; unpublished data), PC12 cells (Plummer et al., 1989), certain sensory neurons (Aosaki and Kasai, 1989), and sympathetic neurons (Plummer et al., 1989; Jones and Jacobs, 1990). In contrast, L-type channels contribute substantial I_{Ba} in some populations of sensory neurons (Scroggs and Fox, 1991) and certain CNS neurons (Mogul and Fox, 1991; Regan et al., 1991).

Our characterization of a novel human neuronal voltage-dependent Ca^{2+} channel firmly establishes the existence of multiple subtypes of DHP-sensitive L-type Ca^{2+} channels. Furthermore, this human neuronal Ca^{2+} channel appears to have functional and pharmacological properties distinct from any other recombinant Ca^{2+} channel expressed to date. Together with the evidence for differentially processed mRNAs encoding three subunits of voltage-dependent Ca^{2+} channels, these results indicate that the molecular diversity of this ion channel class is much greater than previously proposed by traditional biophysical and pharmacological studies.

script is designated α_{2c}. The β gene product expressed in skeletal muscle is designated β_1; the β transcript expressed in neuronal tissues is differentially processed to produce β_2 and β_3 transcripts. An additional β transcript expressed in aorta is designated β_4.

cDNA Libraries

Recombinant cDNA libraries were prepared, and individual cDNA clones were characterized essentially as previously described by Ellis et al. (1988). Unless otherwise noted, the nucleotide numbers in the text refer to cDNA coding sequence. For the isolation of human neuronal α_{1D} subunit cDNAs, RNA was isolated from the human neuroblastoma IMR32 cell line (ATCC #CCL127), which had been grown in 1.0 mM dibutyryl cAMP for 10 days. Four different cDNA libraries were constructed into the phage vector λgt11: oligo(dT)-primed double-stranded cDNA, 1-3 kb size fractionated by agarose gel electrophoresis; oligo(dT)-primed double-stranded cDNA, 3-9 kb size fractionated; random-primed double-stranded cDNA, >1.8 kb; and specifically primed (nucleotides 2417-2446 of α_{1D}) double-stranded cDNA, >1.5 kb. Human neuronal α_{2b} subunit cDNAs were isolated from a human basal ganglia cDNA library (ATCC #37433) and a human brain stem cDNA library (ATCC #37432). Human brain β_2 and β_3 subunit cDNAs were isolated from a human hippocampus cDNA library constructed in the λ phage vector λZAPII (Stratagene, La Jolla, CA, #936205).

Isolation of Recombinant cDNAs Encoding Different Ca^{2+} Channel Subunits

α_{1D} Subunit
Approximately 1×10^6 recombinants of the 1-3 kb library were screened with the rabbit skeletal muscle α_1 subunit cDNA (Ellis et al., 1988). Clone $\lambda\alpha$1.36 (nucleotides 2347-3771 of α_{1D}) was isolated and characterized, and the insert was used to screen the 3-9 kb library. Clone $\lambda\alpha$1.80 (nucleotides 1573-5958) was isolated and characterized, and the 3' portion of the insert was used to screen the random-primed library from which clone $\lambda\alpha$1.163 (nucleotides 4690-7125) was isolated. The 5' portion of α1.80 was subsequently used to screen the random-primed library, resulting in the isolation of clone $\lambda\alpha$1.144 (nucleotides −510 to 1921). The 5' portion of α1.80 was then used to screen the specifically primed library from which clone $\lambda\alpha$1.136 (nucleotides 1117-2478) was isolated.

α_{2b} Subunit
Human genomic α_2 clones were isolated to use as α_2-specific probes of human neuronal cDNA libraries. A rabbit skeletal muscle α_{2b} cDNA fragment, clone SkMCaCHα2.2, comprising nucleotides 43-272 (Ellis et al., 1988), was used to identify and clone two α_2-specific, human genomic EcoRI fragments, HGCaCHα2.20 (3.5 kb) and HGCaCHα2.9 (3.0 kb). Restriction mapping and DNA sequencing revealed that HGCaCHα2.20 contains an 82 bp exon (nucleotides 96-177 of the human α_{2b} coding sequence) and that HGCaCHα2.9 contains 105 bp of an exon (nucleotides 178-282 of the coding sequence). These restriction fragments were used to screen the human basal ganglia cDNA library. HBCaCHα2.1 was isolated (nucleotides −6 to 1129) and used to screen the human brain stem cDNA library. Two clones were isolated, HBCaCHα2.5 (nucleotides −34 to 1128) and HBCaCHα2.8 (nucleotides 680-1528 followed by 1600 nucleotides of intervening sequence). HBCaCHα2.8 was used to rescreen the brain stem library and to isolate HBCaCHα2.11 (nucleotides 845-3566).

β_2 and β_3 Subunits
A rabbit skeletal muscle β_1 subunit cDNA fragment (Ellis et al., 1988; Ruth et al., 1989) was used to screen the human hippocampus cDNA library. Two clones, $\lambda\beta$1 and $\lambda\beta$4, were isolated that appear to encode alternative splice products of the human β subunit transcript expressed in the brain, β_2 and β_3, respectively. $\lambda\beta$1 begins at nucleotides 69 and extends 107 nucleotides beyond the translation stop codon, encoding 1367 nucleotides of coding sequence. $\lambda\beta$1 also contains a 448 nucleotide intron between nucleotides 1146 and 1147 of the coding sequence. $\lambda\beta$4 begins at nucleotide 246 of the coding sequence and diverges from β_2 at nucleotide 1333 as described in the Results. $\lambda\beta$1 was used to

rescreen the hippocampus cDNA library from which clone $\lambda\beta$1.18 was isolated, characterized, and determined to encode nucleotides 1-325 of the β_2 coding sequence.

PCR Analysis
PCR analyses were performed essentially as described by Innis et al. (1990). IMR32 cell cytoplasmic RNA was prepared as described by Ausubel et al. (1988). For the analysis of the series of 5' methionine codons in the α_{1D} cDNA, four oligonucleotide primers were synthesized (numbered in the 5' to 3' orientation): (1) nucleotides −39 to −18, beginning 39 nucleotides 5' of the first methionine codon; (2) nucleotides 58-81; (3) nucleotides 164-187; and (4) nucleotides 314-291. The oligonucleotide pairs (1, 4), (2, 4), and (3, 4) were used to prime PCR assays of cytoplasmic RNA and human genomic DNA. PCR amplification of human genomic DNA and IMR32 cytoplasmic RNA with oligonucleotide pairs (2, 4) and (3, 4) gave the predicted size product (260 and 150 bp, respectively). The cytoplasmic RNA assayed with the pair (1, 4) gave the predicted size product (350 bp); a PCR product of genomic DNA primed with the pair (1, 4) was not detected. The lack of a PCR product primed with pair (1, 4) on genomic DNA suggested the possible presence of an intron between oligonucleotides 1 and 2 and indicated that the positive results with the RNAs could not be due to genomic DNA contamination of the RNA preparations. The cytoplasmic RNA PCR product of the (1, 4) oligonucleotide pair was cloned and sequenced.

Construction of Full-Length cDNAs
α_{1D} Subunit
pVDCCIII(A) was constructed using α1.144 (nucleotides −184 to 1222), α1.136 (nucleotides 1222-2157), α1.80 (nucleotides 2157-4784), and α1.163 (nucleotides 4784-7125). PCR analysis of the α_{1D} transcript revealed that α1.80 contained a 148 nucleotide deletion (nucleotides 2474-2621). To correct this deletion, PCR was performed on IMR32 RNA, and the AccI-BglII fragment (nucleotides 2254-3380) was isolated and used to replace the α1.80 fragment.
α_{2b} Subunit
pHBCaCHα_{2b}(A) was constructed using HBCaCHα2.5 (nucleotides −34 to 1027) and HBCaCHα2.11 (nucleotides 1027-3566).
β_2 Subunit
To construct pHBCaCHβ_{2b}.RBS(A), the 448 nucleotide intron of $\lambda\beta$1 first was deleted via site-directed mutagenesis (Sambrook et al., 1989). $\lambda\beta$1 was subcloned into M13mp19. The mutagenic oligonucleotide was the sense strand of β_2 encoding nucleotides 1128-1165. The final construct was designated pβ1(−). pHBCaCH-β_{2b}.RBS(A) then was constructed using $\lambda\beta$1.18 (nucleotides 1-282) and pβ1(−) (nucleotides 282-1547). The 5' untranslated sequence in $\lambda\beta$1.18 was replaced with an efficient ribosomal-binding site so that the sequence reads 5'-GAATTC (EcoRI) ACCACC (ribosomal-binding site) ATG (start codon) ... −3'. Each α_{1D}, α_{2b}, and β_2 full-length construct was subcloned into pcDNA1 (Invitrogen, San Diego, CA).

Expression Studies in Xenopus Oocytes
In vitro transcripts of human neuronal α_{1D}, α_{2b}, and β_2 subunit cDNAs were synthesized according to the instructions of the mCAP mRNA Capping Kit (Stratagene, La Jolla, CA, #200350). Each plasmid first was linearized by restriction digestion: pVDCCIII(A) with XhoI, pHBCaCHα_{2b}(A) with XhoI, and pHBCaCHβ_{2b}.RBS(A) with EcoRV. T7 RNA polymerase was used to transcribe each cDNA. Xenopus laevis oocytes were dissociated and defolliculated by collagenase treatment and maintained in 100 mM NaCl, 2 mM KCl, 1.8 mM CaCl$_2$, 1 mM MgCl$_2$, 5 mM HEPES (pH 7.6), 20 μg/ml ampicillin, and 25 μg/ml streptomycin at 19°C-25°C for 2-5 days after injection and prior to recording. Oocytes were injected with 6 ng of each in vitro synthesized mRNA species per cell in a volume of 50 nl and were assayed by the two-electrode voltage-clamp method (Dascal, 1987) using the pClamp (Axon Instruments) software package in conjunction with a Labmaster 125 kHz data acquisition interface (Scientific Solutions) to generate voltage commands and to acquire and analyze data. Current signals were digitized at 1-5 kHz and filtered appropriately. I_{Ba}

was recorded in a solution intended to minimize currents carried through K^{+}, Cl^{-}, or Na^{+} channels (Snutch et al., 1990): 40 mM BaCl₂, 36 mM tetraethylammonium chloride, 2 mM KCl, 5 mM 4-aminopyridine, 0.15 mM niflumic acid, 5 mM HEPES (pH 7.6). Currents were leak subtracted by the P/n method provided in pClamp, where n was −4 or −6. Drugs were applied directly into the 60 μl bath while the perfusion pump was turned off. Bay K 8644 and nifedipine were prepared fresh from stock solutions (in dimethyl sulfoxide) and diluted into the bath solution. The dimethyl sulfoxide concentration of the final drug solutions in contact with the cell never exceeded 0.1%. Control experiments showed that 0.1% dimethyl sulfoxide had no effect on membrane currents. ω-CgTx was prepared in a 15 mM BaCl₂ bath solution plus 0.1% cytochrome C (Sigma) (Feldman et al., 1987) to serve as a carrier protein. Control experiments showed that cytochrome C had no effect on currents. Before and during ω-CgTx application, test pulses were recorded at 20 s intervals from the holding potential (−90 mV or −50 mV) to the peak I_{Ba} (−10 mV to 10 mV). To reduce the inhibition of ω-CgTx binding by divalent cations (McCleskey et al., 1987), recordings were made in 15 mM BaCl₂, 73.5 mM tetraethylammonium chloride, and the remaining ingredients identical to the 40 mM Ba²⁺ recording solution.

Acknowledgments

References

Ahlijanian, M. K., Westenbroek, R. E., and Catterall, W. A. (1990). Subunit structure and localization of dihydropyridine-sensitive calcium channels in mammalian brain, spinal cord, and retina. Neuron 4, 819–832.

Aosaki, T., and Kasai, H. (1989). Characterization of two kinds of high-voltage-activated Ca-channel currents in chick sensory neurons. Pflügers Arch. 414, 150–156.

Ausubel, F. M., Brent, R., Kingston, R. E., Moore, D. D., Seidman, J. G., Smith, J. A., and Struhl, K. (1988). Preparation and analysis of RNA. In Current Protocols in Molecular Biology (New York: John Wiley & Sons), pp. 4.1.4.

Bause, E. (1983). Structural requirements of N-glycosylation of proteins. Studies with proline peptides as conformational probes. Biochem. J. 209, 331–336.

Bean, B. P. (1984). Nitrendipine block of cardiac calcium channels: high-affinity binding to the inactivated state. Proc. Natl. Acad. Sci. USA 81, 6388–6392.

Bean, B. P. (1989). Classes of calcium channels in vertebrate cells. Annu. Rev. Physiol. 51, 367–384.

Biel, M., Ruth, P., Bosse, E., Hullin, R., Stühmer, W., Flockerzi, V., and Hofmann, F. (1990). Primary structure and functional expression of a high voltage activated calcium channel from rabbit lung. FEBS Lett. 269, 409–412.

Campbell, K. P., Leung, A. T., and Sharp, A. H. (1988). The biochemistry and molecular biology of the dihydropyridine-sensitive calcium channel. Trends Neurosci. 11, 425–430.

Carbone, E., Sher, E., and Clementi, F. (1990). Ca currents in human neuroblastoma IMR32 cells: kinetics, permeability and pharmacology. Pflügers Arch. 416, 170–179.

Dascal, N. (1987). The use of Xenopus oocytes for the study of ion channels. CRC Crit. Rev. Biochem. 22, 317–387.

Dascal, N., Snutch, T. P., Lübbert, H., Davidson, N., and Lester,

H. A. (1986). Expression and modulation of voltage-gated calcium channels after RNA injection in Xenopus oocytes. Science 237, 1147–1150.

Ellis, S. B., Williams, M. E., Ways, N. R., Brenner, R., Sharp, A. H., Leung, A. T., Campbell, K. P., McKenna, E., Koch, W. J., Hui, A., Schwartz, A., and Harpold, M. M. (1988). Sequence and expression of mRNAs encoding the α₁ and α₂ subunits of a DHP-sensitive calcium channel. Science 241, 1661–1664.

Feldman, D. H., Olivera, B. M., and Yoshikami, D. (1987). Omega Conus geographus toxin: a peptide that blocks calcium channels. FEBS Lett. 214, 295–300.

Fox, A. P., Nowycky, M. C., and Tsien, R. W. (1987). Kinetic and pharmacological properties distinguishing three types of calcium currents in chick sensory neurones. J. Physiol. 394, 149–172.

Glass, D. B., El-Maghrabi, M. R., and Pilkis, S. J. (1986). Synthetic peptides corresponding to the site phosphorylated in 6-phosphofructo-2-kinase/fructose-2,6-bisphosphatase as substrates of cyclic nucleotide-dependent protein kinases. J. Biol. Chem. 261, 2987–2993.

Hess, P. (1990). Calcium channels in vertebrate cells. Annu. Rev. Neurosci. 13, 337–356.

Holz, G. G., Dunlap, K., and Kream, R. M. (1988). Characterization of the electrically evoked release of substance P from dorsal root ganglion neurons: methods and dihydropyridine sensitivity. J. Neurosci. 8, 463–471.

Hui, A., Ellinor, P. T., Krizanova, O., Wang, J.-J., Diebold, R. J., and Schwartz, A. (1991). Molecular cloning of multiple subtypes of a novel rat brain isoform of the α₁ subunit of the voltage-dependent calcium channel. Neuron 7, 35–44.

Innis, M. A., Gelfand, D. H., Sninsky, J. J., and White, T. J. (1990). PCR Protocols: A Guide to Methods and Applications (San Diego, California: Academic Press), pp. 3–27.

Jay, S. D., Ellis, S. B., McCue, A. F., Williams, M. E., Vedvick, T. S., Harpold, M. M., and Campbell, K. P. (1990). Primary structure of the γ subunit of the DHP-sensitive calcium channel from skeletal muscle. Science 248, 490–492.

Jay, S. D., Sharp, A. H., Kahl, S. D., Vedvick, T. S., Harpold, M. M., and Campbell, K. P. (1991). Structural characterization of the dihydropyridine-sensitive calcium channel α₂-subunit and the associated δ peptides. J. Biol. Chem. 266, 3287–3293.

Jones, S. W., and Jacobs, L. S. (1990). Dihydropyridine actions on calcium currents of frog sympathetic neurons. J. Neurosci. 10, 2261–2267.

Koch, W. J., Ellinor, P. T., and Schwartz, A. (1990). cDNA cloning of a dihydropyridine-sensitive calcium channel from rat aorta. J. Biol. Chem. 265, 17786–17791.

Kozak, M. (1987). An analysis of 5′-noncoding sequences from 699 vertebrate messenger RNAs. Nucl. Acids Res. 15, 8125–8132.

Llinás, R., Sugimori, M., Lin, J. W., and Cherksey, B. (1989). Blocking and isolation of a calcium channel from neurons in mammals and cephalopods utilizing a toxin fraction (FTX) from funnel-web spider poison. Proc. Natl. Acad. Sci. USA 86, 1689–1693.

McCleskey, E. W., Fox, A. P., Feldman, D. H., Cruz, L. J., Olivera, B. M., Tsien, R. W., and Yoshikami, D. (1987). ω-Conotoxin: direct and persistent blockade of specific types of calcium channels in neurons but not muscle. Proc. Natl. Acad. Sci. USA 84, 4327–4331.

Mikami, A., Imoto, K., Tanabe, T., Niidome, T., Mori, Y., Takeshima, H., Narumiya, S., and Numa, S. (1989). Primary structure and functional expression of the cardiac dihydropyridine-sensitive calcium channel. Nature 340, 230–233.

Miller, R. J. (1987). Multiple calcium channels and neuronal function. Science 235, 46–52.

Mogul, D. J., and Fox, A. P. (1991). Evidence for multiple types of Ca²⁺ channels in acutely isolated hippocampal CA3 neurones of the guinea-pig. J. Physiol. 433, 259–281.

Mori, Y., Friedrich, T., Kim, M.-S., Mikami, A., Nakai, J., Ruth, P.,

Bosse, E., Hofmann, F., Flockerzi, V., Furuichi, T., Mikoshiba, K., Imoto, K., Tanabe, T., and Numa, S. (1991). Primary structure and functional expression from complementary DNA of a brain calcium channel. Nature 350, 398–402.

Numa, N., and Noda, M. (1986). Molecular structure of sodium channels. Ann. NY Acad. Sci. 479, 338–355.

Perez-Reyes, E., Kim, H. S., Lacerda, A. E., Horne, W., Wei, X., Rampe, D., Campbell, K. P., Brown, A. M., and Birnbaumer, L. (1989). Induction of calcium currents by the expression of the α_1-subunit of the dihydropyridine receptor from skeletal muscle. Nature 340, 233–236.

Perez-Reyes, E., Wei, X., Castellano, A., and Birnbaumer, L. (1990). Molecular diversity of L-type calcium channels. J. Biol. Chem. 265, 20430–20436.

Plummer, M. R., Logothetis, D. E., and Hess, P. (1989). Elementary properties and pharmacological sensitivities of calcium channels in mammalian peripheral neurons. Neuron 2, 1453–1463.

Regan, L. J., Sah, D. W. Y., and Bean, B. P. (1991). Ca^{2+} channels in rat central and peripheral neurons: high-threshold current resistant to dihydropyridine blockers and ω-conotoxin. Neuron 6, 269–280.

Regulla, S., Schneider, T., Nastainczyk, W., Meyer, H. E., and Hofmann, F. (1991). Identification of the site of interaction of the dihydropyridine channel blockers nitrendipine and azidopine with the calcium-channel α_1 subunit. EMBO J. 10, 45–49.

Ruth, P., Röhrkasten, A., Biel, M., Bosse, E., Regulla, S., Meyer, H. E., Flockerzi, V., and Hofmann, F. (1989). Primary structure of the β subunit of the DHP-sensitive calcium channel from skeletal muscle. Science 245, 1115–1118.

Sambrook, J., Fritsch, E. F., and Maniatis, T. (1989). Molecular Cloning: A Laboratory Manual (Cold Spring Harbor, New York: Cold Spring Harbor Laboratory).

Sanguinetti, M. C., and Kass, R. S. (1984). Voltage-dependent block of calcium channel current in the calf cardiac Purkinje fiber by dihydropyridine calcium channel antagonists. Circ. Res. 55, 336–348.

Scroggs, R. S., and Fox, A. P. (1991). Distribution of dihydropyridine and ω-conotoxin-sensitive calcium currents in acutely isolated rat and frog sensory neuron somata: diameter-dependent L channel expression in frog. J. Neurosci. 11, 1334–1346.

Snutch, T. P., Leonard, J. P., Gilbert, M. M., Lester, H. A., and Davidson, N. (1990). Rat brain expresses a heterogeneous family of calcium channels. Proc. Natl. Acad. Sci. USA 87, 3391–3395.

Suzuki, N., and Yoshioka, T. (1987). Differential blocking action of synthetic ω-conotoxin on components of Ca^{2+} channel current in clonal GH3 cells. Neurosci. Lett. 75, 235–239.

Swandulla, D., Carbone, E., and Lux, H. D. (1991). Do calcium channel classifications account for neuronal calcium channel diversity? Trends Neurosci. 14, 46–51.

Tanabe, T., Takeshima, H., Mikami, A., Flockerzi, V., Takahashi, H., Kangawa, K., Kojima, M., Matsuo, H., Hirose, T., and Numa, S. (1987). Primary structure of the receptor for calcium channel blockers from skeletal muscle. Nature 328, 313–318.

Tanabe, T., Beam, K. G., Powell, J. A., and Numa, S. (1988). Restoration of excitation-contraction coupling and slow calcium current in dysgenic muscle by dihydropyridine receptor complementary DNA. Nature 336, 134–139.

Tsien, R. W., Lipscombe, D., Madison, D. V., Bley, K. R., and Fox, A. P. (1988). Multiple types of neuronal calcium channels and their selective modulation. Trends Neurosci. 11, 431–438.

Woodgett, J. R., Gould, K. L., and Hunter, T. (1986). Substrate specificity of protein kinase C use of synthetic peptides corresponding to physiological sites as probes for substrate recognition requirements. Eur. J. Biochem. 161, 177–184.

Yeager, R., Yoshikami, D., Rivier, J., Cruz, L. J., and Miljanich, G. P. (1987). Transmitter release from electric organ nerve terminals: blockade by the calcium channel antagonist, omega Conus toxin. J. Neurosci. 7, 2390–2396.